

**GAS PHASE BENZENE HYDROGENATION ON A  
NICKEL-SILICA CATALYST**

Promotor: Prof.Dr.Ir. J.W.E. Coenen.

**GAS PHASE BENZENE HYDROGENATION ON A  
NICKEL-SILICA CATALYST**

**PROEFSCHRIFT**

**TER VERKRIJGING VAN DE GRAAD VAN DOCTOR IN DE  
WISKUNDE EN NATUURWETENSCHAPPEN AAN DE KATHO-  
LIEKE UNIVERSITEIT TE NIJMEGEN, OP GEZAG VAN DE  
RECTOR MAGNIFICUS PROF. MR. F.J.F.M. DUYNSTEE  
VOLGENS BESLUIT VAN HET COLLEGE VAN DECANEN  
IN HET OPENBAAR TE VERDEDIGEN OP VRIJDAG  
18 APRIL 1975 DES NAMIDDAGS TE 4 UUR**

**DOOR**

**ROELAND ZEGER CUCHULAIN VAN MEERTEN**

**GEBOREN TE NIJMEGEN**

**1975**

**DRUK: STICHTING STUDENTENPERS NIJMEGEN**

**Ik dank hierbij allen die hun medewerking hebben verleend aan de totstandkoming van dit proefschrift.**

# TABLE OF CONTENTS

	INTRODUCTION . . . . .	1
Chapter I	EXPERIMENTAL DATA AND PHENOMENOLOGICAL DESCRIPTION	
	Abstract . . . . .	2
	Introduction . . . . .	2
	Experimental Methods . . . . .	3
	Results . . . . .	5
	Discussion . . . . .	10
	Acknowledgement . . . . .	12
	References . . . . .	12
Chapter II	GRAVIMETRIC EXPERIMENTS ON BENZENE, CYCLOHEXENE AND CYCLOHEXANE ADSORPTION AND BENZENE HYDROGENATION	
	Abstract . . . . .	14
	Introduction . . . . .	14
	Experimental Methods . . . . .	16
	Results . . . . .	17
	Discussion . . . . .	22
	References . . . . .	26
Chapter III	LOW-FIELD MAGNETIZATION EXPERIMENTS ON HYDROGEN, BENZENE, CYCLOHEXENE AND CYCLOHEXANE ADSORPTION AND BENZENE HYDROGENATION	
	Abstract . . . . .	27
	Introduction . . . . .	27
	Experimental Methods . . . . .	31
	Results and Discussion . . . . .	33
	Acknowledgement . . . . .	48
	Appendix . . . . .	48
	References . . . . .	49
Chapter IV	RATE EQUATIONS AND CURVE FITTING	
	Abstract . . . . .	51
	Introduction . . . . .	51
	Derivation of the Rate Equations . . . . .	52
	Computer Curve Fitting . . . . .	57
	Discussion . . . . .	57
	List of Symbols . . . . .	66
	References . . . . .	67
	APPENDIX: Entropies of Benzene and Hydrogen Adsorbed on Nickel, and their Standard States . . . . .	69
	SUMMARY . . . . .	76
	SAMENVATTING . . . . .	78
	STELLINGEN . . . . .	80
	CURRICULUM VITAE . . . . .	82



## INTRODUCTION

Already in the beginning of our century Sabatier and Senderens hydrogenated benzene to cyclohexane on finely powdered nickel. Nowadays this reaction is of industrial importance for the production of pure cyclohexane, an intermediate in the manufacture of nylon-6 and nylon-6,6 (1). Since no analytical problems arise in the separation of product cyclohexane and reactant benzene, the hydrogenation of benzene is attractive as a test reaction for hydrogenation catalysts containing group VIII metals. In our laboratory the reaction was used to test the kinetic behaviour of nickel-silica catalysts with varying crystallite size at temperatures from 25 up to 85°C (2). For this range of temperature a simple mechanism was proposed, which did, however, not apply to data obtained at higher temperatures.

In the literature no consensus of opinion exists about the mechanism of the benzene hydrogenation, and experimental data of different investigators are often contradictory. We therefore have measured reaction rates of the benzene hydrogenation on a nickel-silica catalyst over a range of experimental conditions as broad as possible.

In this thesis data on the benzene hydrogenation are presented from three experimental methods: a kinetic (chapter I), a gravimetric (chapter II), and a magnetic (chapter III) method. On the basis of these data a number of reaction mechanisms were derived and tested (chapter IV). From statistical thermodynamics the entropy of benzene and hydrogen adsorbed on the metal surface was estimated. The values are compared with values obtained from computer curve fitting.

1. Kirk-Othmer, *Encyclopedia of Chem. Techn.* Vol.3, Wiley and Sons Inc., New York, 1964.
2. Coenen, J.W.E., van Meerten, R.Z.C., and Rijntjen, H.T., *Proc. Int. Congr. Catal.*, 5th (Palm Beach, FL) 1972 1, 671 (1973).

Gas Phase Benzene Hydrogenation on a  
Nickel-Silica Catalyst

I. EXPERIMENTAL DATA AND PHENOMENOLOGICAL DESCRIPTION

R.Z.C. van Meerten and J.W.E. Coenen

*Department of Catalysis, Faculteit der Wiskunde en Natuurwetenschappen,  
Katholieke Universiteit, Toernooiveld, Nijmegen, The Netherlands*

(Accepted for publication in Journal of Catalysis  
Received November 2, 1973; revised July 11, 1974)

ABSTRACT.

The hydrogenation of benzene on a nickel-silica catalyst was measured in a differential flow reactor with glc analysis of the reaction products.

The parameters varied over wide intervals. The order of reaction with respect to hydrogen rose from 0.5 at 25°C to 2-3 at 200°C. The order of reaction with respect to benzene rose from about 0.1 at 25°C to 0.3-0.5 at 200°C. No inhibition of cyclohexane could be detected. The apparent activation energies in the temperature range 25-120°C decreased from 12.5 kcal/mol at 600 Torr hydrogen pressure to 11.7 kcal/mol at 75 Torr. At higher temperatures a maximum appeared in the reaction rate. Depending on hydrogen pressure (75-600 Torr) the temperature of the maximum shifted from 135 to 180°C. Neither poisoning, nor diffusion limitation, nor approach to equilibrium could account for the maximum.

INTRODUCTION

Although much work has been done on the kinetics of benzene hydrogenation on nickel, there is still no consensus of opinion on kinetic behavior and mechanism. We should note that in most published investigations a narrow range of experimental conditions was explored. Mechanisms based on such limited data are generally not applicable to conditions outside the explored range, nor can



they be considered to be unique within the range. We therefore decided to vary experimental parameters to a greater extent, hoping thus to arrive at a unique and more generally applicable mechanism. The present paper presents the experimental data we obtained in gas phase hydrogenation with hydrogen pressures between 0.1 and 1 atm and temperatures between 20 and 250°C. Measurements at higher pressures are in progress and will be published in due course.

If we take a comprehensive look at the vast but fragmented kinetic evidence from the literature, it appears at first sight conflicting, but certain trends in reported reaction orders may be noted. At temperatures below 100°C many authors (1,3,4,6-8,10,13,15,18) report reaction orders in hydrogen pressure between 0.5 and 0.7. At higher temperatures the order in hydrogen rises to values from 1 to 2.5 (7,10,15,18), ultimately reaching a value of 3 at 200°C (21).

In many papers (1,3,4,6,9,13,14,20) a near zero order in benzene pressure is reported, sometimes increasing from a low value of 0.1-0.3 at temperatures below 100°C (7,8,10,11,15,17,18) to about 0.5 at temperatures between 150 and 250°C (7,10,15,18,21). An inhibiting effect of cyclohexane is reported by some (7,9,13) and denied by others (10,11,15,17,21).

With respect to apparent activation energies there is again considerable variation but with some trends discernible. In the temperature region below 180°C on nickel films values of 7-9 kcal mol<sup>-1</sup> are reported (2,3,14) as well as a value of 12 kcal mol<sup>-1</sup> (16). On supported catalysts apparent activation energies ranging from 9 to 16 kcal mol<sup>-1</sup> are variously reported (1,4,6-8,10,11,13,15,17-20).

Near 180°C the reaction rate reaches a maximum ( $E_{app}=0$ ), as is mentioned for nickel by Herbo (9), Germain et al. (7) and Nicolai et al. (15) and for ruthenium and other metals by Kubicka (12). The phenomenon may also be observed in the data of Taylor (19). Beyond 200°C the rate falls with increasing temperature ( $E_{app}$  negative) as shown by Herbo (9), Nicolai et al. (15) and Zlotina and Kiperman (21). No firm mechanistic explanation of this maximum has been given. It has been qualitatively ascribed to poisoning (15) or to decrease in reactant adsorption (7,9).

## EXPERIMENTAL METHODS

The *reactants* hydrogen and benzene were purified following the methods given elsewhere (4). The nickel-on-silica *catalyst* (code NZ 10) containing 11.3% Ni was reduced in the reactor for 4 hr at 450°C with 600 liters (STP) hr<sup>-1</sup> (g cat)<sup>-1</sup>

flowing through the catalyst bed. The degree of reduction was 90%, the nickel surface area was  $26.2 \text{ m}^2 (\text{g cat})^{-1}$ , and the crystallite size from  $D=4310/S_{\text{Ni}}$  (see Refs.(4,5)) was  $15.1 \text{ \AA}$ . The total BET area ( $\text{N}_2$ ) was  $222 \text{ m}^2 (\text{g cat})^{-1}$ , the mean pore radius  $108 \text{ \AA}$  (from BET pore volume and surface area), and the particle diameter about  $10 \text{ \mu m}$  (from Coulter counter and microscopy).

*Apparatus* (Fig.1). The gas phase hydrogenation was performed in a differential flow reactor. The reactor consisted of a glass tube with a porous glass disk (4, 7 or 10 mm diameter) on which the catalyst was loaded. The reactant flow pressed the catalyst particles on the porous glass disk. Different quantities of catalyst were used. At temperatures below  $70^\circ\text{C}$  about 100 mg catalyst was used in the reactor of 10 mm diameter (catalyst bed height, 4.5 mm). Samples of 3 to 10 mg (catalyst bed diameter, 4 mm; height, 1 to 3 mm) were used above  $70^\circ\text{C}$  depending on the applied hydrogen pressure. Reaction temperature was measured with an uncovered copper-constantan thermocouple (diameter of wires, 0.15 mm). The couple was not catalytically active in the benzene hydrogenation. The reduction treatment at  $450^\circ\text{C}$  did not affect the properties of the couple.

The reaction system of glass, consisting of a series connected benzene saturator (6), condenser (7), fixed bed differential reactor (8), gas-liquid chromatography (glc) sampling valve (9) and cold trap (10), was enclosed between two precision needle valves (I and II). The entry valve (I) was connected to a constant pressure high purity hydrogen source, the exit valve (II) to a vacuum line. Adjustment of valves (I) and (II) determined flow and pressure in the system. Constant flow and constant reactor pressure were maintained by a magnetic valve (III), bypassing needle valve (II) and controlled by a photoelectric sensor (3) on one of the arms of the mercury manometer (4). Thus the difference in pressure between the reference vessel (2) and the exit of the system was held within 1 Torr.

The flow of the incoming hydrogen was measured with a soap film flow meter. The saturator (6) and condenser (7) were thermostated, the latter at  $10\text{--}20^\circ\text{C}$  lower temperature than the former, ensuring the saturation pressure for benzene. At the fixed condenser temperature of  $18.55^\circ\text{C}$ , the benzene partial pressure was always 70.0 Torr at the exit of the condenser. The benzene pressure could be diminished by the partial bypassing of the saturator and condenser with hydrogen via needle valve (IV). The reactor equipped with a preheater spiral was also thermostated. The degree of conversion was obtained after 15 min stabilization of the flow from glc analysis of the reactor effluent (Becker research gas chromatograph type 3810, carbowax column, catharometer detection,

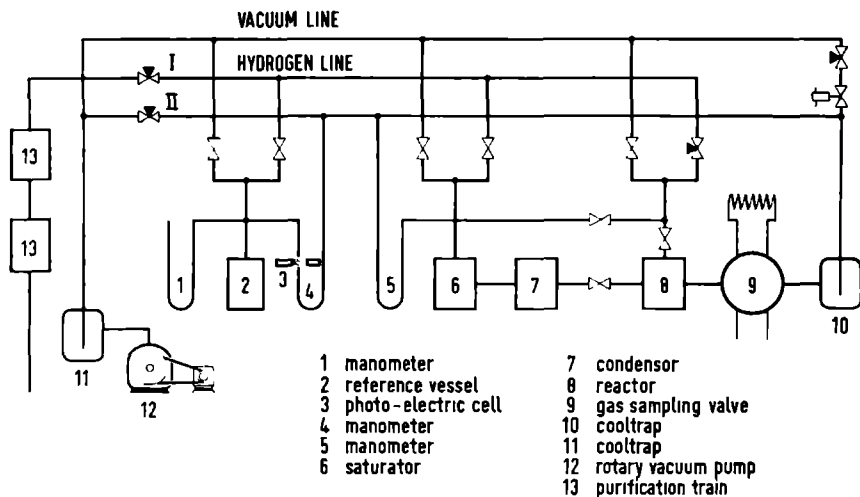


Fig.1. Apparatus for gas phase benzene hydrogenation below atmospheric pressure.

Kipp & Zonen integrator BC 1). Benzene partial pressure was determined from the ratio of surface areas of the peaks on the recorder of the gas chromatograph, using as standard the 70 Torr benzene peak. A correction was made for the pressure drop over the catalyst bed, as measured by manometer (5), to obtain the benzene pressure at the entrance of the reactor. Mercury contamination of the catalyst was avoided by placing the manometers downstream, except manometer (5) for a few seconds per measurement. Hydrogenation conditions: hydrogen pressure, 75-600 Torr; benzene pressure, 1-70 Torr; cyclohexane pressure, 0-50 Torr; temperature, 20-250°C. Reaction rates are expressed per unit nickel area in micromoles of  $H_2$  per minute per square meter. Conversions were in general kept below 4%.

## RESULTS

The hydrogenation of benzene to cyclohexane on the nickel-silica catalyst was measured as a function of temperature and partial pressures of hydrogen, benzene and cyclohexane. Sets of measurements were made with the rate being observed at standard conditions before and after every set. In a set the reaction temperature was decreased and/or increased, giving the same reaction rate

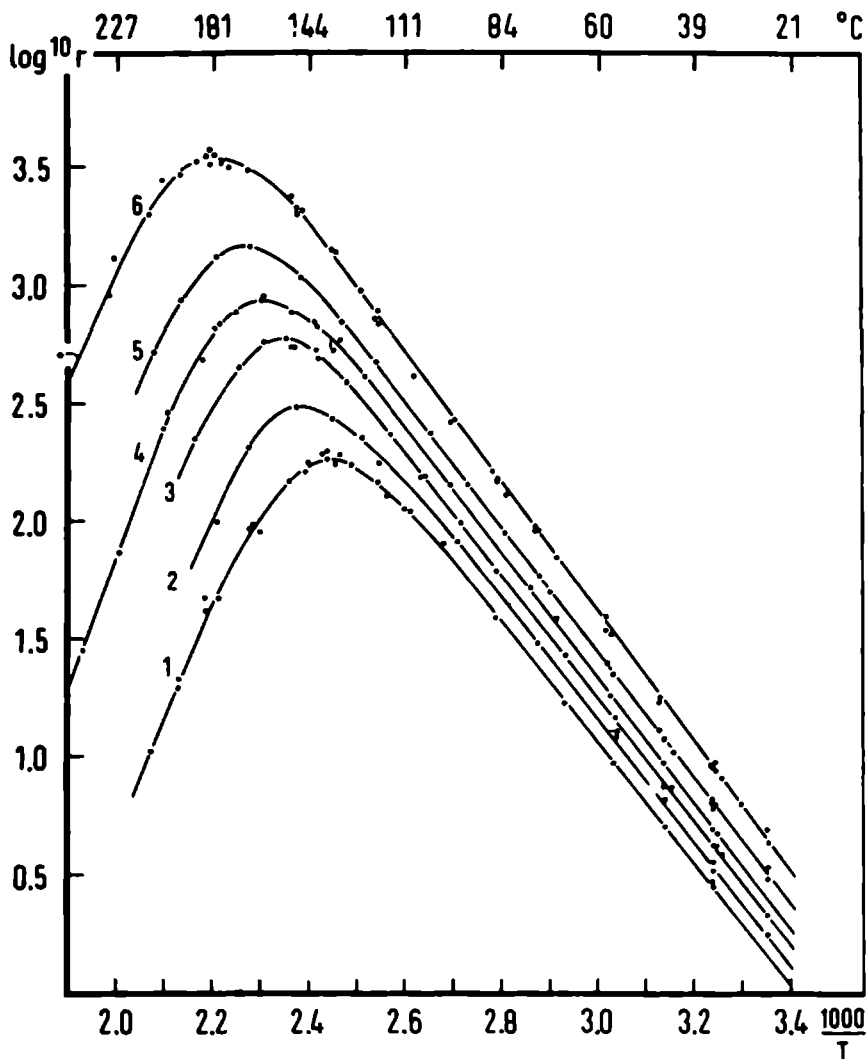


Fig.2. Arrhenius plots, showing the effect of temperature and hydrogen partial pressure on rate of benzene hydrogenation. Reaction rate  $r$  ( $\mu\text{mol H}_2 \text{ min}^{-1} \text{ m}^{-2}$ ). For the curves indicated by 1,2,3,4,5,6 the hydrogen pressures were 75,100,150,200,300,600 Torr, respectively ; benzene partial pressure, 70 Torr.

at the same temperature and pressures. Reaction rates were reproducible within  $\pm 4\%$ .

The effects of temperature and hydrogen pressure are shown by the Arrhenius plots in Fig.2. The plots are linear below  $110^\circ\text{C}$  and yield values for  $E_{\text{app}}$ , which increase slightly with hydrogen pressure from  $11.7 \text{ kcal mol}^{-1}$  at 75 Torr to  $12.5 \text{ kcal mol}^{-1}$  at 600 Torr. Well-defined maxima in the reaction rate shift from  $135^\circ\text{C}$  at 75 Torr to  $180^\circ\text{C}$  at 600 Torr. The apparent activation energy beyond the maximum reaches a value of about  $-23 \text{ kcal mol}^{-1}$ , in agreement with Zlotina and Kiperman (21), who found  $-22 \text{ kcal mol}^{-1}$ .

From the exponential rate expression  $r = k \cdot p_{\text{H}_2}^n \cdot p_{\text{B}}^m \cdot p_{\text{cy}}^q$ , the formal reaction orders  $n$  in hydrogen,  $m$  in benzene and  $q$  in  $\text{C}_6\text{H}_{12}$  cyclohexane are derived by means of logarithmic plots; as the plots are not strictly linear, the orders are functions of the partial pressures involved. Figure 3 shows the effect of hydrogen pressure and temperature (data of Fig.2) and in Fig.4 the order in

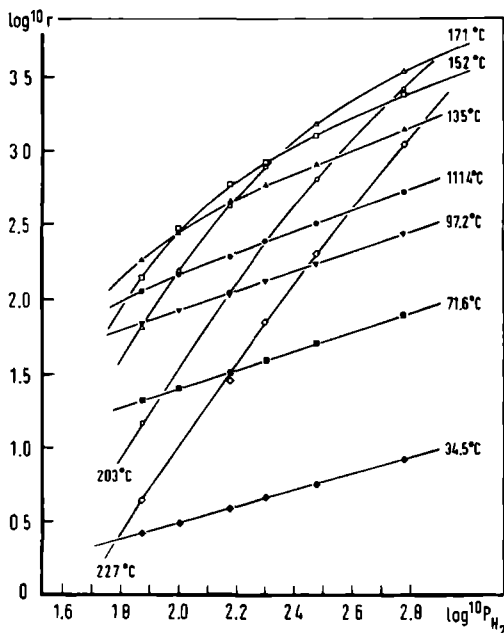


Fig.3. Rate of benzene hydrogenation as a function of hydrogen partial pressure (from Fig.2) ; pressures (Torr).

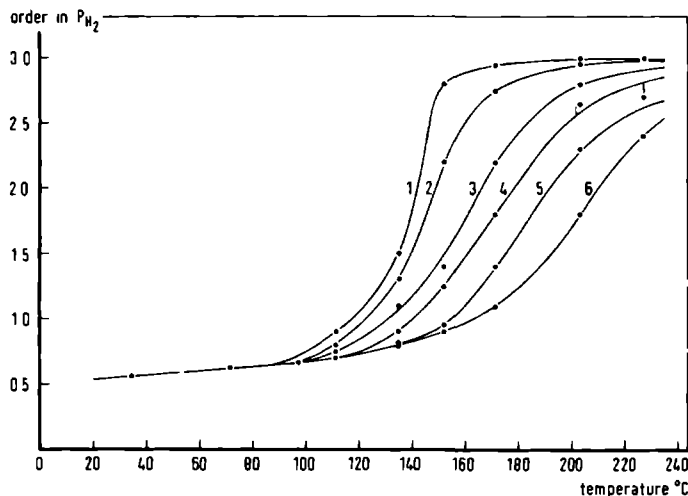


Fig.4. Order of reaction in hydrogen pressure as a function of temperature and hydrogen partial pressure (from Fig.3). For the curves indicated by 1,2,3,4,5,6 the hydrogen pressures were 75,100,150,200,300,600 Torr, respectively.

hydrogen pressure is shown. We note a smooth transition from low order (0.5-0.7) below 100 $^{\circ}C$  to orders in excess of 2 at high temperature. This transition is steeper at lower hydrogen pressure. Figures 5 and 6 show the dependence of the rate on benzene pressure at various temperatures. The order in benzene pressure derived from these data is shown in Fig.7. To gain insight into the effect of cyclohexane partial pressure on the rate, the conversion of benzene to cyclohexane was allowed to reach higher values (up to 70%) and in one experiment cyclohexane was added to the feed. A correction for the decrease in hydrogen and benzene partial pressures was made by integration over the catalyst bed. A factor can be derived to convert the experimental reaction rate at high conversion degrees ( $r_{uncorr}$ ) to the reaction rate at differential conversion ( $r_{corr}$ ). With the ratio of initial pressures  $p_{H_2}^0/p_B^0 = \alpha$  and with the conversion of benzene given by  $x$ , the factor is :

$$\int_0^x \frac{(1+\alpha-3x)^{m+n}}{(1-x)^m \cdot (\alpha-3x)^n} \cdot dx \Big/ \frac{(1+\alpha)^{m+n}}{\alpha^n}$$

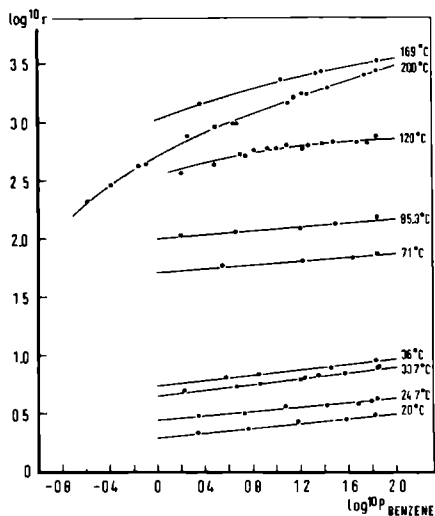


Fig.5. Rate of benzene hydrogenation as a function of benzene pressure (Torr) ;  $p_{\text{H}_2} = 600$  Torr.

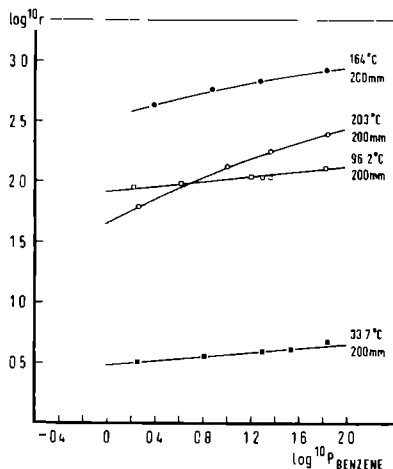


Fig.6. Rate of benzene hydrogenation as a function of benzene pressure (Torr) ;  $p_{\text{H}_2} = 200$  Torr.

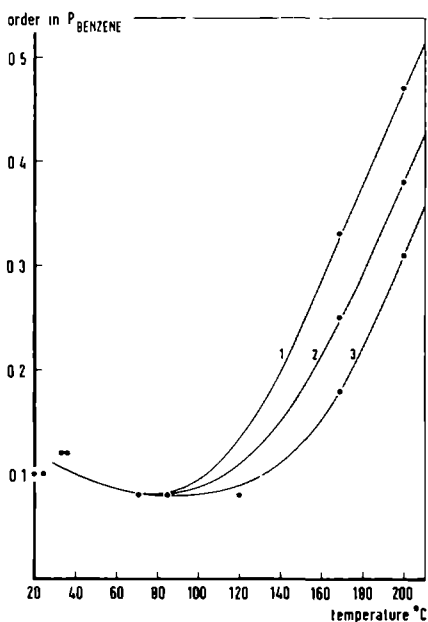


Fig.7. Order of reaction in benzene pressure as a function of temperature and benzene partial pressure (from Fig.5). For the curves indicated by 1, 2, 3 the benzene pressures were 2, 10, 70 Torr, respectively.

TABLE I  
INFLUENCE OF CYCLOHEXANE PRESSURE ON RE-  
ACTION RATE OF BENZENE HYDROGENATION  
 $r$  ( $\mu\text{mol H}_2 \text{ min}^{-1} (\text{m}^2 \text{ Ni})^{-1}$ )

Temp (°C)	$P_{\text{H}_2}^o$	Torr $P_{\text{B}}^o$	$P_{\text{cy}}$	Conv. (%)	$r_{\text{uncorr}}$	Corr. factor	$r_{\text{corr}}$
31.7	600	70	0	4.7	6.46	-	6.46
31.7	600	70	0	14.0	6.34	1.01	6.40
31.7	600	70	0	68.5	6.17	1.05	6.48
31.7	600	70	51	29	5.9	1.02	6.0
31.7	600	70	51	55	5.95	1.03	6.14
103	600	70	0	3.4	392	-	392
103	600	70	0	12.5	379	1.01	383
103	600	70	0	65	336	1.05	353
208	400	70	0	4.6	1001	-	1001
208	400	70	0	21.4	942	1.06	998
208	400	70	0	53	773	1.16	897

The integral was solved graphically for the different conditions. The influence of cyclohexane pressure on the reaction rate can be observed in Table I, the decrease in reaction rate being nearly within the experimental error, so that we conclude that the order  $q$  in cyclohexane is zero between 25 and 200°C. Under our normal hydrogenation conditions no cracking products were found in the reaction products. When we used a catalyst sample of 500 mg at temperatures above 200°C (almost complete conversion of benzene) 1 to 2% cracking product, possibly methane, could be detected.

## DISCUSSION

The general trends which we derived from fragmented and seemingly contradictory literature studies find remarkable confirmation in our experimental data, covering a wide range of conditions. Of special importance is the occurrence of well-defined maxima in the rate vs temperature plots.

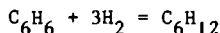
The maxima in the rate of reaction versus temperature curves can be brought about by catalyst poisoning, diffusion limitation or approach to thermodynamic equilibrium. At the higher temperatures poisoning of the surface of the catalyst by organic residues is possible. However, sets of successive measurements were made with increasing and decreasing temperatures, giving the same result, showing that at the higher temperatures no irreversible catalyst deactivation.



occurred. Moreover, standard rates before and after each measuring series were well within experimental error (generally less than 5%). On the other hand, activities at temperatures over the maximum decrease easily by a factor of 10. Also a reversible poisoning at high temperature, disappearing with return to lower temperature, must be excluded: when we decreased very rapidly the reaction temperature, say from 220°C to the temperature of standard measurement 100°C, during a constant flow of benzene over the catalyst, no decrease in standard activity could be detected. Moreover, no cracking products could be detected in the reactor effluent. So poisoning cannot be the reason for a maximum in the reaction rate.

Also diffusion limitation might be a possible cause of rate limitation, although this can never give rise to negative activation energies. The small dimension of the catalyst particles (about 10  $\mu\text{m}$ ) and the large pore radius (108 Å) make the Thiele modulus small, so that even in the worst case (200°C,  $p_{\text{H}_2}$  = 600 Torr and  $p_{\text{B}}$  = 0.7 Torr) the effectiveness factor is very close to 1.

Approach to thermodynamic equilibrium conversion could give rise to limitations in the reaction rate. Equilibrium conversions for the equilibrium,



are shown in Table 2, together with experimental conversions at nearby temperatures. Even at the highest temperatures and lowest pressures the dehydrogenation of cyclohexane plays no part in our experiments. We therefore believe our rate data to be real over the entire range of conditions. A satisfactory mechanistic description of benzene hydrogenation should be able to describe this behavior.

TABLE 2  
THERMODYNAMICS OF THE REACTION  
 $\text{C}_6\text{H}_6 + 3\text{H}_2 = \text{C}_6\text{H}_{12}$

Temp (°C)	$K_p^a$	$p_{\text{H}_2}/p_{\text{B}}$	$p_{\text{total}}$ (Torr)	Equil. conv. (%)	Exp. conv. (%)
265	4.9	9	760	77	0.94
252	16.2	3	270	20	0.58
227	186	1	150	9.5	0.51

<sup>a</sup> Calculated from data given in Ref.(22).

In principle the appearance of a maximum is not entirely unexpected: the increase with temperature of the rate constant(s) for the surface reaction(s) will be counteracted by a decreased degree of occupation of the catalyst surface with reactants. Provided the activation energy for the surface reaction and heats of adsorption of the reactants have the right relationship a maximum can occur. This argument was already used in earlier studies (7,9). In an earlier publication (4) we found that a very simple mechanism, involving a stepwise addition of adsorbed hydrogen atoms to adsorbed benzene, the second addition being rate determining, described our earlier data on liquid phase benzene hydrogenation below 100°C very satisfactorily. However, this mechanism is entirely unsuitable to describe the present more extensive data. Especially the occurrence of maximum rates cannot be fitted into our earlier description. We are making progress with two mechanisms proposed by Snagovskii et al. (18), both involving a stepwise addition of adsorbed hydrogen atoms to adsorbed benzene. One involves a slow step, the position of which is an adjustable parameter; the other involves a series of slow steps with equal rate constants. Both rate equations predict a maximum in the rate with temperature. The experimental data of (18) do not reach the temperature for maximum rate. We are now fitting the above experimental data to these mechanisms and will publish the results in due course.

#### ACKNOWLEDGMENT

The measurements were performed with great care by the research students J.M.B. Balvert, A.C.M. Verhaak and T.F.M. de Graaf.

#### REFERENCES

1. Aben, P.C., Platteeuw, J.C., and Stouthamer, B., *Proc. Int. Congr. Catal.*, 4th (Moscow) 1968 1, 395 (1971) (Pap. 31).
2. Anderson, J.R., *Austr. J. Chem.* 10, 409 (1957).
3. Beeck, O., and Ritchie, A.W., *Discuss. Faraday Soc.* 8, 159 (1950).
4. Coenen, J.W.E., van Meerten, R.Z.C., and Rijnten, H.T., *Proc. Int. Congr. Catal.*, 5th (Palm Beach, FL) 1972 1, 671 (1973).
5. Coenen, J.W.E., and Linsen, B.G., in "Physical and Chemical Aspects of Adsorbents and Catalysts" (Linsen, B.G., Ed.), p.497. Academic Press, New York, 1970.
6. Dixon, G.M., and Singh, K., *Trans. Faraday Soc.* 65, 1128 (1969).
7. Germain, J.E., Maurel, R., Bourgeois, Y., and Sinn, R., *J. Chim. Phys.* 60, 1219, 1227 (1963).
8. Hartog, F., Tebben, J.H., and Zwietering, P., *Actes 2ème Congr. Int. Catal.*, 1960 1, 1229 (1961).
9. Herbo, C., *Bull. Soc. Chim. Belg.* 50, 257 (1941).

10. Jiracek, F., Pasek, J., and Horak, J., *Collect. Czech. Chem. Commun.* 33, 3266 (1968).
11. Kehoe, J.P.G., and Butt, J.B., *J. Appl. Chem. Biotechnol.* 22, 23 (1972).
12. Kubicka, H., *J. Catal.* 12, 223 (1968).
13. Lyubarskii, G.D., *Actes 2ème Congr. Int. Catal.*, 1960 1, 1242 (1961).
14. Madden, W.F., and Kemball, C., *J. Chem. Soc.* 54, 302 (1961).
15. Nicolai, J., Martin, R., and Jungers, J.C., *Bull. Soc. Chim. Belg.* 57, 555 (1948).
16. Van der Plank, P., thesis, Leiden, 1968.
17. Roethe, K.P., Roethe, A., Rosahl, B., and Gelbin, D., *Chem.-Ing.-Tech.* 42, 805 (1970).
18. Snagovskii, Y.S., Lyubarskii, G.D., and Ostrovskii, G.M., *Kinet. Catal. (USSR)* 7, 232 (1966).
19. Taylor, W.F., *J. Catal.* 9, 99 (1967).
20. Völter, J., Lange, B., and Kuhn, W., *Z. Anorg. Allg. Chem.* 340, 253 (1965).
21. Zlotina, N.E., and Kiperman, S.L., *Kinet. Catal. (USSR)* 8, 337, 1129 (1967).
22. Janz, G.J., "Thermodynamic Properties of Organic Compounds." Academic Press, New York, 1967.

Gas Phase Benzene Hydrogenation on a  
Nickel-Silica Catalyst

II. GRAVIMETRIC EXPERIMENTS ON BENZENE, CYCLOHEXENE AND  
CYCLOHEXANE ADSORPTION AND BENZENE HYDROGENATION

R.Z.C.van Meerten, A.C.M. Verhaak and J.W.E. Coenen

*Department of Catalysis, Faculteit der Wiskunde en Natuurwetenschappen,  
Universiteit van Nijmegen, Toernooiveld, Nijmegen, The Netherlands*

ABSTRACT

Experiments of benzene adsorption on a nickel-silica catalyst suggested three forms of chemisorption, covering only part of the surface: a) a reactive form being the active form in normal benzene hydrogenation, in our experiments discernable up to 110°C, b) a form of low reactivity not contributing to normal benzene hydrogenation, removable by several hours hydrogen flow at the temperature of adsorption, c) a dissociatively adsorbed form, occurring at high temperatures (above 120°C) only if hydrogen was not present during adsorption. This last form acted as a poison for the hydrogenation reaction and was removed by hydrogen at 400°C only.

Physical adsorption of benzene as a function of temperature and benzene pressure was measured.

Cyclohexane adsorbed in hydrogen atmosphere (30-200°C) appeared to be easily removable by hydrogen.

INTRODUCTION

In a preceding paper (1) we gave rate data for the hydrogenation of benzene on a 10% nickel-silica catalyst, code NZ 10. This work was purely phenomenological and only a few possible mechanisms were mentioned. The results arrived at by many authors, each of them investigating a narrow range of parameters with seemingly conflicting results, agreed with the data we obtained for

the hydrogenation of benzene on nickel, measured over a much wider range.

Before fitting postulated mechanisms to our data by means of a computer program, we would like to have more insight into the events taking place on the surface of our catalyst. Since the results published in the literature may be expected to be specific for every catalyst, we investigated adsorption and reaction phenomena on our NZ 10 catalyst in two systems: a gravimetric system with a Cahn electrobalance to determine benzene and cyclohexane adsorption under different conditions (this paper), and an AC-permeameter according to Selwood to measure changes in the magnetization of the superparamagnetic nickel catalyst NZ 10, resulting from adsorption of hydrogen, benzene, cyclohexene and cyclohexane (2). In the gravimetric determination of the quantity of chemisorbed benzene on a metal-support catalyst, the problem arises of physisorption on support and metal next to chemisorption on the metal. The physisorbed quantity is easily removed by evacuation ( $10^{-4}$  Torr) of the sample. Chemisorbed species remain on the metal surface (2).

Since Moyes and Wells (3) have recently reviewed benzene chemisorption on different metals, we will mention only papers dealing with nickel catalysts. Shopov et al. (4) studied the adsorption of benzene and cyclohexane at room temperature with IR and EPR-spectroscopy in combination with gravimetric adsorption measurements. By hydrogen they could remove about 2/3 of the chemisorbed benzene and less than half of the cyclohexane. Both hydrocarbons covered only part of the surface. It led them to the conclusion that there are different active centers for the interaction of the hydrocarbons with nickel. (De)hydrogenation was supposed to take place on one of these sites and hydrocarbon deposition on the other.

In experiments with  $C^{14}$  labeled benzene on different nickel catalysts Tetenyi et al. (5) also found a partial coverage by benzene. A maximum in the adsorbed quantity of benzene occurred between 140 and 160°C. Chemisorbed benzene could be fully removed only by hydrogen (for a small part in the form of benzene, the remainder as cyclohexane), part of it was exchangeable with gaseous benzene. No poisoning of the (de)hydrogenation reaction occurred. Up to 200°C they could not detect cyclohexane adsorption.

Tetenyi's reversibly adsorbed benzene may be in a  $\pi$ -adsorbed form, a concept introduced by Garnett et al. (6). However, Erkelens et al. (7) working with IR-spectroscopy on nickel-silica catalyst could not detect species of a  $\pi$ -adsorbed form: a broad band in the spectrum pointed to a mixture of adsorbed species with a range of C-H vibrations, apparently indicating that benzene had lost its aromatic character.

Most of the experimental work so far implies adsorption of benzene on a hydrogen-free surface, which gives indications for different adsorption forms. Important for the elucidation of the mechanism of the benzene hydrogenation, however, is the question how and to what extent benzene and cyclohexane adsorb on a catalyst in a hydrogen atmosphere. The present paper deals with this problem.

## EXPERIMENTAL METHODS

In Ref.(9) we described the purification of hydrogen and benzene. Nitrogen, cyclohexane and cyclohexene were purified in similar ways.

The *catalyst* (code NZ 10) contained 11.3% nickel, the nickel surface area was  $26.2 \text{ m}^2(\text{g cat})^{-1}$ , total BET ( $\text{N}_2$ ) area was  $222 \text{ m}^2(\text{g cat})^{-1}$ . The reduction time was 4 hr at  $450^\circ\text{C}$ , the evacuation took 2 hr at  $450^\circ\text{C}$  and  $10^{-4}\text{Torr}$ . For further details see Ref.(1).

The heart of the *gravimetric flow system* consisted of a Cahn electrobalance (2550 RH Ventron Instr.Corp.), shown in Fig.1. It was connected with the glass flow system described earlier (1). Weight changes were registered with  $10 \mu\text{g}$  precision on a Kipp BD 6 recorder. The reactant flow was brought in a few millimeters above the catalyst bed, which consisted of a thin layer spread over the bottom of a glass basket. The temperature of the reference and sample basket was kept constant up to  $75^\circ\text{C}$  by a waterbath, at higher temperatures by an electrical furnace. Reduction of the catalyst was performed in situ at  $450^\circ\text{C}$ . When the temperature of reference and sample basket was not the same, a buoyancy correction had to be taken into account. Weight registration in vacuo proved impossible because of unknown forces, probably electrostatic, a phenomenon that persisted when the hang-down tubes were immersed in electrically earthed salt water. Already at rather low gas pressures these effects were avoided: at 20 Torr gas pressure of nitrogen or hydrogen a "zero level" was taken arbitrarily. The electrical measuring part of the balance was kept free from benzene vapour by means of a gasstream of nitrogen or hydrogen along the suspension wires. The temperature of the catalyst could only be measured a few millimeters above the catalyst bed. To test the balance, flow and static measurements were done without catalyst in the system, with different gases (hydrogen, nitrogen, hydrogen with benzene and nitrogen with benzene) at temperatures from 20 to  $200^\circ\text{C}$ . The buoyancy effects were tabulated. In all experiments samples of 200 mg catalyst NZ 10 were used and corrections for buoyancy were made. In most experiments a benzene vapour pressure of 70 Torr, the saturation value at  $18.5^\circ\text{C}$ , was used.

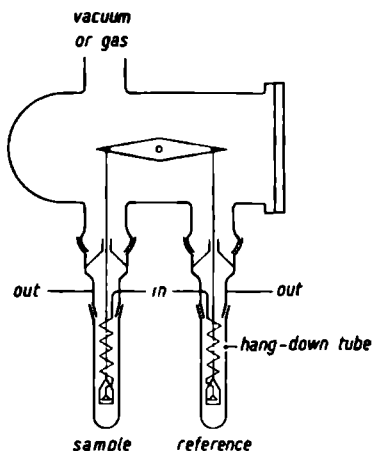


Fig.1. Experimental setup for gravimetric measurements.

## RESULTS

The sensitivity of the electrobalance was insufficient to measure changes in hydrogen adsorption above 20 Torr. Nitrogen adsorption was measured at different temperatures (e.g. 110  $\mu\text{g}$  at 30°C on 200 mg cat., decreasing at higher temperatures) and these values were used for corrections in relevant hydrocarbon adsorption measurements.

Under flow conditions of specified benzene pressure, physical adsorption on the silica support and nickel metal takes place. Therefore, the physical adsorbed quantities had to be removed by either evacuation or nitrogen flow, before we were able to measure chemisorption of benzene. By this procedure chemisorbed benzene was not removed as was ascertained by magnetic measurements (2).

### *Benzene Chemisorption on a Hydrogen-free Catalyst*

Nitrogen (670 Torr), nitrogen with benzene (600, 70 Torr respectively, for  $\frac{1}{2}$  hr) and nitrogen (670 Torr) were led over a hydrogen-free catalyst sample. At five temperatures the chemisorption of benzene was measured on the same sample (Table 1). The degree of occupation by benzene ( $\theta_B$ ) was calculated with a surface area for benzene of 41  $\text{\AA}^2$  (4,10). The coverage of the metal surface was only partial and seemed to have a maximum at 150°C. Above 110°C the benzene adsorption became time-dependent. Reduction at 450°C between the measure-

TABLE 1  
BENZENE CHEMISORPTION  
ON NICKEL-SILICA CATALYST NZ10 (200 mg)  
WITH A HYDROGEN-FREE SURFACE

Temp (°C)	Amount benzene chemisorbed ( $\mu\text{g}$ )		Degree of occu- pation $\theta_B$
	Exposure $\frac{1}{2}$ hr	Exposure 1 hr	
28	450		0.27
59	290		0.17
60 <sup>a</sup>	500-600		0.3-0.36
105	410		0.24
153	690		0.42
		750	0.45
196	490		0.30
		600	0.36

<sup>a</sup> Fresh sample

ments at the different temperatures removed all the adsorbed hydrocarbons. On a fresh catalyst sample we could not reproduce the 59°C value, we found 500-600  $\mu\text{g}$  instead. The lower values are possibly due to a sintering of the catalyst by the repeated reduction and evacuation for longer times and higher temperatures than in the later experiments.

The reactivity of benzene adsorbed on a hydrogen-free sample was investigated by subsequent exposure to hydrogen of a pressure of 600 Torr. From the 590  $\mu\text{g}$  benzene adsorbed at 60°C about 400  $\mu\text{g}$  was removed by a hydrogen flow within one hour at 25°C.

#### *Benzene Chemisorption on a Catalyst Partially Occupied with Hydrogen*

By hydrogen adsorption and evacuation during 15 min to  $5 \times 10^{-4}$  Torr at the temperature of the following benzene adsorption, the catalyst was partially occupied with hydrogen. The degree of coverage by the remaining hydrogen is not the same at the different temperatures. The results of the benzene adsorption in a nitrogen atmosphere on the catalyst partially precovered by hydrogen are given in Table 2. The quantity benzene adsorbed at temperatures below 120 °C was about 600  $\mu\text{g}$ , at 200°C about 1000  $\mu\text{g}$ . In this set of experiments it was also found that benzene adsorption at high temperature is time-dependent, e.g. at 202°C about 100  $\mu\text{g}$  per hr on 200 mg catalyst.

Hydrogen admission to the catalyst partially covered by benzene and hydrogen immediately started the hydrogenation of benzene, but there was a different



TABLE 2  
BENZENE CHEMISORPTION  
ON NICKEL-SILICA CATALYST NZ10 (200 mg)  
PARTIALLY COVERED WITH HYDROGEN

Temp (°C)	Amount benzene chemisorbed ( $\mu\text{g}$ )			$R^a$ ( $\mu\text{g min}^{-1}$ )	$r^b$ ( $\mu\text{mol H}_2 \text{ m}^{-2} \text{ min}^{-1}$ )
	exposure $\frac{1}{2}$ hr ( $p_{\text{H}_2} = 0$ Torr)	after an injection of hydrogen ( $p_{\text{H}_2} = 20$ Torr)	after $\frac{1}{2}$ hr hydrogen flow ( $p_{\text{H}_2} = 700$ Torr)		
34	570		160	100	6.7
60	680		200	100	
104	500	400	300	100	
144	740	720	400	10	5.7
196	1000	1020	700	10	5.1
202	1250 <sup>c</sup>	1200	750	10	3.8

<sup>a</sup>  $R$  is the reactivity of the chemisorbed benzene with the first hydrogen flowing over the catalyst.

<sup>b</sup>  $r$  is the activity after the adsorption procedure and the hydrogen flow ( $\frac{1}{2}$  hr).  $r$  relates to the conditions: temp, 31°C;  $p_{\text{H}_2} = 600$  Torr;  $p_{\text{B}} = 70$  Torr. The standard activity at these conditions was  $6.8 \mu\text{mol H}_2 \text{ m}^{-2} \text{ min}^{-1}$ .

<sup>c</sup> Benzene was flowed over the catalyst for 2 hr.

behaviour in reactivity  $R$  between benzene adsorbed at high or low temperature, but not in the reaction products. From glc analysis it appeared that after admission of hydrogen almost all the benzene left the surface in the form of cyclohexane. Half an hour hydrogen flow didn't remove all the adsorbed species, a poisoning of the surface active under standard conditions occurred. The benzene adsorbed at low temperature was totally removable after one night in hydrogen atmosphere. The fraction of benzene adsorbed at high temperatures not removable by the normal hydrogen treatment could be removed only by hydrogen at 400°C.

#### *Benzene Chemisorption during the Reaction with Hydrogen (30–150°C)*

Hydrogen (600 Torr) and benzene (70 Torr) were led over the catalyst. Sudden evacuation diminished the hydrogen pressure, almost stopped the reaction (order with respect to hydrogen pressure 0.6) and removed physisorbed benzene. For measuring benzene chemisorption a hydrogen pressure of 20 Torr had to be established, but then the reaction proceeded immediately. Consequently an extrapolation to the moment of hydrogen admission had to be carried out. The results

TABLE 3  
BENZENE CHEMISORPTION  
ON NICKEL-SILICA CATALYST NZ10 (200 mg)  
DURING REACTION WITH HYDROGEN <sup>a</sup>

Temp (°C)	Amount benzene chemisorbed (μg)	
	after evacuation ( $p_{H_2}=20$ Torr)	after $\frac{1}{2}$ hr hydrogen flow ( $p_{H_2}=670$ Torr)
25		200
25	670	130
31		300
32	600	300
59	400	200
110 <sup>b</sup>		200

<sup>a</sup>  $p_{H_2} = 600$  Torr;  $p_B = 70$  Torr.

<sup>b</sup> Temperature of catalyst is about 40°C higher, see text.

are tabulated in Table 3.

Next a hydrogen flow at a pressure of 700 Torr was led over the catalyst for  $\frac{1}{2}$  hr. Under these conditions a faster desorption of benzene (as cyclohexane and benzene as was determined from glc analysis) occurred at higher temperatures. About 1/3 to 1/2 of the adsorbed benzene remained on the surface. This not-reactively adsorbed quantity was the same if no evacuation procedure was applied, e.g. in the experiments at 25 and 31°C (Table 3).

At temperatures above 60°C the degree of conversion became too high, so that the rise in temperature of the sample due to the heat of reaction could no longer be controlled and was higher than measured directly. The amount of physical adsorption can give an indication for the real temperature inside the catalyst particle. From the experiments concerning the physical adsorption of benzene in nitrogen atmosphere (Table 4) it can be derived that in the experiment at 110°C (Table 3) the temperature difference between catalyst and surrounding gas was about 40°C. So we found that at 150°C only 200 μg was not-reactively adsorbed.

#### *Physical Adsorption of Benzene*

On catalyst NZ 10 we measured the amount of physical adsorption:

- a) in nitrogen atmosphere as a function of temperature, Table 4
- b) during reaction of benzene with hydrogen from 30-150°C, Table 4

TABLE 4  
PHYSICAL ADSORPTION OF BENZENE  
ON NICKEL-SILICA CATALYST NZ10 (200 mg) <sup>a</sup>

Temp (°C)	Physisorbed benzene in nitrogen atmosphere (μg)	Number of monolayers	Physisorbed benzene in hydrogen atmosphere <sup>b</sup> (μg)
32	20500	1.45	19600
60	8100	0.57	7200
112	1700	0.12	500
152	700	0.05	
195	0	0	

<sup>a</sup>  $p_B = 70$  Torr.

<sup>b</sup> During reaction with hydrogen  $p_{H_2} = 600$  Torr.

TABLE 5  
PHYSICAL ADSORPTION OF BENZENE  
ON NICKEL-SILICA CATALYST NZ10 (200 mg)  
DURING BENZENE HYDROGENATION AT 30°C  
AS A FUNCTION OF BENZENE PRESSURE <sup>a</sup>

$p_B$ (Torr)	Physisorbed benzene (μg)	Number of monolayers	$r$ (μmol H <sub>2</sub> m <sup>-2</sup> min <sup>-1</sup> )
70	21200	1.50	6.30
21	9800	0.70	5.61
4.8	2800	0.20	4.5
1.93	850	0.06	-

<sup>a</sup>  $p_{H_2} = 600$  Torr.

c) as a function of benzene pressure during reaction at 30°C, Table 5.

In all cases a correction was made for the chemisorbed quantity of benzene.

The number of monolayers was calculated from the BET surface of the catalyst, 222 m<sup>2</sup>(g cat)<sup>-1</sup> and a surface area of a benzene molecule of 41 Å<sup>2</sup>.

#### *Adsorption of Cyclohexane in a Hydrogen Atmosphere*

In these experiments hydrogen was led over a freshly reduced catalyst, followed by hydrogen with cyclohexane (at pressures of 600 resp. 70 Torr), next the sample was evacuated, hydrogen was admitted up to 20 Torr and finally hydrogen was flowed over at a pressure of 600 Torr for 20 min. The results are given in Table 6.

TABLE 6  
CYCLOHEXANE ADSORPTION  
ON NICKEL-SILICA CATALYST NZ10 (200 mg)  
IN A HYDROGEN ATMOSPHERE <sup>a</sup>

Temp (°C)	Physisorbed cyclohexane (µg)	Chemisorbed cyclohexane (µg)	
		after evacuation (P <sub>H<sub>2</sub></sub> =20 Torr)	after 20 min hydrogen flow
33	15200	50	0
73	3400	100	0
107	1350	100	0
140	650		0
172	400	300	150
205	400		50

<sup>a</sup> P<sub>cy</sub> = 70 Torr; P<sub>H<sub>2</sub></sub> = 600 Torr

At low temperatures no cyclohexane remained on the surface after flowing over hydrogen. At higher temperatures, however, a stronger adsorption occurred. The 150 µg cyclohexane that remained on the catalyst at 172°C after flowing over hydrogen during 20 min, was removed by a hydrogen flow during 2 hr at 200°C.

*Adsorption of Cyclohexane on a Catalyst Partially Covered with Hydrogen*

In one experiment we evacuated a hydrogen covered catalyst sample at 35°C, flowed over the catalyst respectively nitrogen (670 Torr), nitrogen with cyclohexane (600 resp. 70 Torr) and nitrogen (670 Torr). The resulting adsorption of cyclohexane was 450 µg / 200 mg cat. After a hydrogen flow for ½ hr at the same temperature, about 150 µg still remained on the surface. This quantity proved to be removed from the surface after one night under 1 atm hydrogen pressure.

*Adsorption of Cyclohexene on a Catalyst Partially Covered with Hydrogen*

In one experiment 760 µg cyclohexene was adsorbed on 200 mg catalyst in nitrogen atmosphere at 34°C. The same procedure as described above for cyclohexane was used.

DISCUSSION

The experiments described above concerned in the first place the adsorption and reactivity of benzene on a nickel-silica catalyst. Before benzene was adsorbed, the hydrogen coverage of the samples was zero in the experiments shown

in Table 1, partial and depending on temperature of evacuation in the experiments shown in Table 2, while almost full coverage had been established in the experiments shown in Table 3.

#### *Adsorption of Benzene at Temperatures below 110°C*

Benzene was adsorbed in an amount of 500-700  $\mu\text{g}$  (Tables 1,2,3) independent of the hydrogen coverage. Assuming a surface area for benzene of  $41 \text{ \AA}^2$  (4,10), the degree of coverage of benzene is 0.3-0.4. This result is not unexpected for a catalyst with a mean nickel particle diameter of  $15 \text{ \AA}$ , where the fit of molecules requiring  $41 \text{ \AA}^2$  will hardly be such that all nickel surface atoms can be covered. However, in the work of others (4,5,8) involving larger crystallites benzene adsorption was also found to be limited to a partial occupation. The fact that at temperatures below  $110^\circ\text{C}$ , the benzene coverage appears largely independent of the hydrogen coverage on the same surface, points to a larger heat of adsorption of benzene than of hydrogen on that part of the surface. This means for the reaction mechanism of benzene hydrogenation, that benzene and hydrogen have their "own" part of the surface and that to a first approximation their adsorptions may be considered non-competitive.

#### *Reactivity of Benzene Adsorbed below 110°C*

We observed that within a half hour about 2/3 of benzene chemisorbed below  $110^\circ\text{C}$  at various hydrogen coverages was reactive with hydrogen. The same quantity was found by Shopov et al. (4) on a clean surface at  $25^\circ\text{C}$ . The other part of the adsorbed benzene was much less reactive. This difference in reactivity of benzene with hydrogen points to different forms of adsorption. Possibly a  $\pi$ -adsorbed form exists next to a  $\sigma$ -bonded type, the  $\pi$ -form being reactive via Rooney's mechanism (12), the  $\sigma$ -form being slowly reactive.

#### *Adsorption and Reactivity of Benzene Adsorbed at Temperatures above 110°C*

At temperatures above  $110^\circ\text{C}$  benzene adsorption is time-dependent (Table 1,2), in contrast to the low temperature adsorption, and takes place on a larger part of the surface.

As is shown in Table 2, the reactivity of the adsorbed benzene with hydrogen under a pressure of 20 to 700 Torr appeared to be quite different for the species adsorbed at low or high temperatures. In normal benzene hydrogenation (1) the reaction rate at  $200^\circ\text{C}$  was in the order of  $1000 \mu\text{mol H}_2 \text{ m}^{-2}\text{min}^{-1}$ , but here at  $200^\circ\text{C}$  the rate at which the adsorbed benzene disappeared from the surface was about  $0.1 \mu\text{mol H}_2 \text{ m}^{-2}\text{min}^{-1}$ , equivalent to  $10 \mu\text{g}$  benzene per minute.

Although the relevant benzene pressure is low for this last reaction rate, there is a high degree of occupation of the nickel surface by benzene. Only part of this benzene could be removed by hydrogen, in contrast with the desorption experiments of Tetenyi et al.(5) at 150°C, where only a small fraction was not reactive. The quantity of hydrocarbons remaining on the surface after hydrogen treatment (Table 2) gradually increased with temperature, possibly because at higher temperatures more hydrogen was pumped off before the adsorption of benzene than at lower temperatures. At 200°C an irreversible adsorption form, probably dissociated  $\text{CH}_2^-$ ,  $\text{CH}_3^-$ -species (7) or nickel carbides (11) can occupy part of the surface active in the benzene hydrogenation at standard conditions (31°C,  $p_{\text{H}_2}$  = 600 Torr,  $p_{\text{B}}$  = 70 Torr), as follows from the decrease in activity at these conditions. This was observed on a catalyst sample partially occupied with hydrogen, but in normal benzene hydrogenation (1) we do not find such a decrease in activity at standard conditions. It may be concluded that with hydrogen on the catalyst, a dissociation of benzene is suppressed. This also follows from the data in Table 3, which show that during the reaction of benzene with hydrogen, the not-reactive fraction of adsorbed benzene remains confined to 200  $\mu\text{g}$  / 200 mg cat. up to 150°C. The statement is further confirmed by Martin et al.(11). From measurements of the saturation magnetization of their nickel-silica catalyst they found that above 160°C on a bare surface, benzene formed 24 bonds with nickel. If, on the contrary, benzene was adsorbed on a nickel surface partially covered with hydrogen, benzene cracking was suppressed and the number of bonds was found to be much smaller.

Although in the high temperature adsorption measurements of Table 2 the reactivity of adsorbed benzene is low, the normal hydrogenation at the same temperature proceeds much faster (1). Two possibilities can be discerned: a) if hydrogen is present, active benzene adsorbs in another form on the same surface sites on which benzene adsorbed irreversibly, or b) active benzene adsorbs on other sites but could not be detected in our experiments because it was removed during the nitrogen flow to remove physisorbed benzene. Martins findings (11) indicate that case a) is certainly possible, but in our view case b) looks most probable because after the adsorption/hydrogenation procedure at 196°C given in Table 2, 700  $\mu\text{g}$  of unreactive hydrocarbons remained on the surface of the catalyst, corresponding to a degree of coverage of 0.4. The resulting decrease in activity at standard conditions is only 25%, indicating that only 25% of the active sites have been poisoned. This is an indication that irremovable adsorption takes place for the greatest part on other places than where reaction at 31°C occurs.

As a conclusion we can say that benzene adsorbs in different forms on part of the nickel surface. Three forms of chemisorption can be assigned to benzene:

- a) a reactive form being the active form in the normal benzene hydrogenation, in our experiments discernable up to 110°C.
- b) a form of low reactivity not contributing to the normal benzene hydrogenation.
- c) a dissociatively adsorbed form, only occurring if no hydrogen is present during the adsorption at high temperature; it can act as a poison for the hydrogenation reaction.

#### *Adsorption of Cyclohexane*

In contrast to Tetenyi et al. we found chemisorption of cyclohexane if the adsorption took place without hydrogen in the gasphase. Shopov (4) also found adsorption of cyclohexane at 25°C, but in a smaller quantity than benzene. Half of the adsorbed cyclohexane was not removable by hydrogen according to Shopov. In our experiment some hydrogen was still on the surface when adsorption took place and 2/3 of the adsorbed cyclohexane was then removable by hydrogen.

More important for the elucidation of the mechanism of the benzene hydrogenation is the adsorption of cyclohexane in a hydrogen atmosphere. As is shown in Table 6 no chemisorption occurred up to 172°C. The nonremovable quantity at this temperature can be ascribed to the evacuation after the adsorption, so that a temporary lack of hydrogen dissociated the cyclohexane, since at 205°C on a sample which was not evacuated, the non-removable quantity was only 50 µg. From these data we conclude that in normal benzene hydrogenation cyclohexane is removed quickly and forms no inhibition for benzene adsorption. In (1) it was already found that the order with respect to cyclohexane pressure was zero from 25 to 200°C. The dissociative adsorption of cyclohexane is prevented by hydrogen, as was the case with benzene in the benzene hydrogenation and in the experiments of Martin et al. (11).

In a forthcoming paper (2) dealing with magnetization measurements, the chemisorbed quantities of benzene, cyclohexene and cyclohexane determined by the gravimetric and magnetic methods will be compared.

#### *Physical Adsorption of Benzene*

The physisorbed quantities of benzene on silica and nickel surface (Tables

4 and 5) have not had much attention in literature.

The chemisorbed quantity is small compared to the physisorbed quantity up to 110-150°C. Perhaps this physisorbed benzene acts as a stock from which benzene molecules can be taken to fill vacant chemisorption sites situated especially near the metal-support boundary where only migration over a small distance is needed. This may be the reason why the order with respect to benzene in the benzene hydrogenation is low (about 0.1) up to 120°C (1), and why above this temperature the order increases rapidly with decreasing physically adsorbed benzene to reach a value of about 0.4 at 200°C.

#### REFERENCES

1. Van Meerten, R.Z.C., and Coenen, J.W.E., *J. Catal.*, in press.
2. Van Meerten, R.Z.C., de Graaf, T.F.M., and Coenen, J.W.E., to be published.
3. Moyes, R.B., and Wells, P.B., in "Advances in Catalysis" (D.D.Eley, H.Pines, and P.B.Weisz, Eds.), Vol.23, p.121. Academic Press, New York, 1973.
4. Shopov, D., Palazov, A., and Andreev, A., *Proc. Int. Congr. Catal.*, 4th (Moscow) 1968 1, 388 (1971) (Pap. 30).
5. Tetenyi, P., and Babernics, L., *J. Catal.* 8, 215 (1967).
6. Garnett, J.L., and Sollich-Baumgartner, W.A., in "Advances in Catalysis" (D.D.Eley, H.Pines, and P.B.Weisz, Eds.), Vol.16, p.95. Academic Press, New York, 1966.
7. Erkelens, J., and Eggink-du Burck, S.H., *J. Catal.* 15, 62 (1969).
8. Selwood, P.W., "Adsorption and Collective Paramagnetism." Academic Press, New York, 1962.
9. Coenen, J.W.E., van Meerten, R.Z.C., and Rijntzen, H.T., *Proc. Int. Congr. Catal.*, 5th (Palm Beach, FL) 1972 1, 671 (1973).
10. Moyes, R.B., and Wells, P.B., in "Advances in Catalysis" (D.D.Eley, H.Pines, and P.B.Weisz, Eds.), Vol.23, p.147, Ref.52. Academic Press, New York, 1973.
11. Martin, G.A., and Imelik, B., *Surface Sci.* 42, 157 (1974).
12. Rooney, J.J., *J. Catal.* 2, 53 (1963).



Gas Phase Benzene Hydrogenation on a  
Nickel-Silica Catalyst

III. LOW-FIELD MAGNETIZATION EXPERIMENTS ON HYDROGEN, BENZENE, CYCLO-  
HEXENE AND CYCLOHEXANE ADSORPTION AND BENZENE HYDROGENATION

R.Z.C.van Meerten, T.F.M.de Graaf and J.W.E. Coenen

*Department of Catalysis, Faculteit der Wiskunde en Natuurwetenschappen,  
Universiteit van Nijmegen, Toernooiveld, Nijmegen, The Netherlands*

ABSTRACT

From magnetization-volume isotherms of hydrogen adsorption on a superparamagnetic nickel catalyst evidence was obtained that hydrogen was not distributed homogeneously over crystallites with small differences in diameter.

Adsorption and desorption isotherms did not coincide. A possible cause is an activated slow adsorption on non-metallic nickel.

Magnetization-volume isotherms of benzene, cyclohexene and cyclohexane showed that these hydrocarbons occupied the nickel surface only partially. Only a range in the number of bonds between the hydrocarbons and nickel can be assigned. By evacuation to  $10^{-4}$  Torr physically adsorbed benzene and cyclohexane could be desorbed, chemisorbed species remained on the surface.

Magnetization measurements during the hydrogenation of benzene showed that only a small part of the nickel surface played a part in the reaction and that a weakly bound form of dissociatively adsorbed hydrogen was active in the reaction.

INTRODUCTION

We have given a phenomenological description of the hydrogenation of benzene on a nickel-silica catalyst (NZ 10) over a wide range of conditions in a preceding paper (1). In a second paper dealing with gravimetric adsorption experiments (2) we showed to what extent benzene and cyclohexane adsorbed and were reactive with hydrogen on this same nickel-silica catalyst. In the present

paper we report about measurements of the magnetization of nickel as a function of the degree of occupation by hydrogen, benzene, cyclohexene and cyclohexane.

In the paper about the gravimetric measurements (2) we paid attention to the reactivity of the adsorbed hydrocarbons, in this paper the way of adsorption and the reactivity of the adsorbed hydrogen plays the greater part. Next to adsorption experiments we measured the magnetization during benzene hydrogenation as a function of the hydrogen pressure, to get information about the degree of occupation of the reactants during the hydrogenation process.

We will first deal with some literature data on magnetization of nickel in catalysts as a function of the adsorption of hydrogen and hydrocarbons (4-9).

#### *The Influence of Hydrogen Adsorption on the Magnetization of Nickel*

In high-field experiments Selwood (4) showed that on hydrogen adsorption the decrease in magnetic moment of a surface nickel atom  $\epsilon$  equals 0.71 B.M., independent of temperature, degree of occupation and crystallite size. On the contrary Martin et al. (6) found in high field experiments a temperature dependence of  $\epsilon$

$$\epsilon(T) = \frac{I_{sp}(T^{\circ}K)}{I_{sp}(0^{\circ}K)} \cdot \alpha$$

where  $I_{sp}$  is the spontaneous magnetization and  $\alpha$  a constant of 0.7 B.M., independent of the degree of occupation and crystallite size.

Below 40 Å a dependence of  $\epsilon$  on the crystallite size is found by Knappwost et al. (10). They ascribed it to an influence of the support in their Ni-MgO catalyst.

#### *Benzene and Cyclohexane Adsorption*

Assuming that between one hydrogen molecule and two nickel surface atoms two bonds were formed and that the gases were distributed homogeneously over the nickel crystallites, Selwood (4) found a temperature dependent number of bonds for benzene in low field magnetization measurements from the ratio of the slopes of the magnetization-volume isotherm of hydrogen and benzene: from about 5 bonds at 25°C up to 18 bonds at 200°C. For cyclohexane the number of bonds at 150°C was about 8. In saturation magnetization measurements (the particle size distribution of the catalyst plays no part, in contrast with low-field magnetization measurements), assuming 0.6 B.M. per nickel atom decoupled per bond, Martin et al. (5,18) found that benzene formed 8 bonds at 25°C, 25 at 150°C and still higher values at higher temperatures. For cyclohexane the number of

bonds was 10 at 25°C and 30 at 220°C.

From the comparison of high-and low-field magnetization experiments Martin et al.(6) concluded that hydrogen was distributed homogeneously over the nickel crystallites, but benzene was not. Benzene prefers the smaller crystallites. This explains the difference in number of bonds found by Selwood and Martin.

Selwood (4) found that chemisorbed benzene could occupy only part of the metal surface, as was also found by Shopov et al.(11) in gravimetric and EPR spectroscopy, and by Van Meerten et al.(2) in gravimetric experiments.

The assignment of a number of bonds from magnetization measurements is doubtful for the following three reasons according to Moyes et al.(12):

- a) the possibility for benzene to form a  $\pi$ -bond, with backdonation of electrons from the metal to the antibonding orbitals of benzene.
- b) hydrogen spillover may occur and apply to the hydrogen dissociated from benzene and to the hydrogen added to a sample for measuring a magnetization volume isotherm.
- c) with other coordination numbers of the metal other forms of adsorption are possible.

In low-field magnetization experiments a fourth reason arises, viz. a possible inhomogeneous partition of the gas over the metal crystallite size distribution. The effect is a slope of the MV isotherm different from the case of a homogeneous distribution.

### *Superparamagnetism*

The phenomenon superparamagnetism is described in detail by others (4,7,8, 13,14). It means that we have to do with ferromagnetic single domain particles with a diameter smaller than about 100 Å, in thermodynamic equilibrium with the direction of the applied field (no hysteresis), a behaviour which is similar to paramagnetic atoms, although their magnetic moment is much larger: superparamagnetism.

### *Magnetization-Volume Isotherm*

If a gas adsorbs on a nickel particle, an electronic interaction between gas and metal causes a decrease in magnetic moment of the nickel particle. The decrease in magnetization of the sample as a function of the volume of gas adsorbed can be described in the magnetization-volume isotherm.

For the theoretical description of the magnetization we use the relation derived by Geus and Nobel (8) from the Langevin function for uniform small

(< 30 Å) superparamagnetic particles in a weak magnetic field (< 400 Oe) at 300°K

$$M_0 = \mu_0 N n^2 \beta(T)^2 \mu_B^2 \frac{H}{3kT} \quad \text{eq. (a)}$$

with

$$\beta(T) = \beta(0^\circ\text{K}) \frac{I_{\text{sp}}(T)}{I_{\text{sp}}(0^\circ\text{K})} \quad \text{eq. (b)}$$

in which  $M_0$  is the magnetization at zero coverage ( $\text{amp m}^{-1}$ ),  $N$  the number of metal particles per unit volume catalyst ( $\text{m}^{-3}$ ),  $n$  the number of metal atoms per particle,  $\beta$  the number of Bohr magnetons per metal atom,  $\mu_B$  the magnetic moment of one Bohr magneton ( $\text{J m}^2 \text{wb}^{-1}$ ),  $H$  the external magnetic field strength ( $\text{amp m}^{-1}$ ),  $k$  the Boltzmann constant ( $\text{J } ^\circ\text{K}^{-1}$ ),  $T$  the absolute temperature ( $^\circ\text{K}$ ),  $I_{\text{sp}}$  the spontaneous magnetization with values taken from (15) ( $\text{amp m}^{-1}$ ),  $\mu_0$  equals  $4\pi \times 10^{-7} \text{ wb amp}^{-1} \text{ m}^{-1}$ .

With the assumption that per atom adsorbed the moment of one nickel atom is decoupled, Geus and Nobel derived the following summation for adsorption on a particle size distribution

$$\frac{\Delta M}{M_0} = -1.052 \times 10^{-2} x \frac{\sum_i n_i}{\sum_i s_i} \cdot \frac{\sum_i n_i s_i}{\sum_i n_i^2} + 0.0028 \times 10^{-2} x^2 \left( \frac{\sum_i n_i}{\sum_i s_i} \right)^2 \cdot \frac{\sum_i s_i^2}{\sum_i n_i^2} \quad \text{eq. (c)}$$

with  $s_i$  the number of gas atoms adsorbed by the  $i$ -th particle, which contains  $n_i$  nickel atoms, and  $x$  the number of ml gas adsorbed (STP) per g metal.

For our purpose we will modify formula (c). In the first place our adsorption experiments concerned hydrogen, therefore for the decrease in moment per adsorbed hydrogen atom at  $0^\circ\text{K}$  we use the value measured by Martin et al. (6), 0.7 B.M.. For the oxygen adsorption Geus and Nobel used a value of 0.606 B.M.. The value determined by Martin in saturation magnetization measurements approaches Selwood's  $\epsilon$  of 0.71 B.M., independent of temperature. We prefer Martin's value because his catalyst had a particle size distribution resembling our catalyst NZ 10.

In (16) Coenen et al. described a nickel crystallite as a hemisphere, which they assumed to be the most favourable shape energetically. With a volume of a nickel atom of  $11 \text{ Å}^3$ , an average area per surface nickel atom of  $6.33 \text{ Å}^2$  and  $\theta_i$  the degree of coverage of particle  $i$ , the number of adsorbed atoms on the surface  $s_i$  is

$$s_i = 3.0 n_i^{2/3} \theta_i \quad \text{eq. (d)}$$

Substitution of  $\epsilon = 0.7$  and  $s_i$  in equation (c) gives

$$\frac{\Delta M}{M_0} = -1.215 \times 10^{-2} \times \underbrace{\frac{\sum n_i}{\sum n_i^2} \cdot \frac{\sum n_i^{5/3} \theta_i}{\sum n_i^{2/3} \theta_i}}_{\text{factor A}} + 0.369 \times 10^{-4} \times \underbrace{x^2 \left( \frac{\sum n_i}{\sum n_i^{2/3} \theta_i} \right)^2 \cdot \frac{\sum n_i^{4/3} \theta_i^2}{\sum n_i^2}}_{\text{factor B}} \quad \text{eq. (e)}$$

Four cases can be discerned:

a) uniform particles, equal  $\theta$  for all particles:  $A=1$  and  $B=1$ .

b) uniform particles, unequal  $\theta$ 's :  $A=1$  but  $B \neq 1$ .

As an example we take  $N_1$  particles with  $\theta=\theta$  ,  $N-N_1$  particles with  $\theta=0$ , then  $A=1$  and  $B= N/N_1$  (see also Geus et al.(8)).

c) particle size distribution, equal  $\theta$  for all particles: in  $A$  and  $B$  the  $\theta$ 's cancel.

d) particle size distribution, unequal  $\theta$ 's: no simplification possible.

#### EXPERIMENTAL METHODS

For the measurement of the magnetization of catalyst NZ 10 we used an AC-permeameter largely analogous to the instrument used by Selwood (4). However, our system consisted of *two* primary coils, each containing a secondary coil. The secondary coils were connected thus, that without inserted samples their voltages cancelled each other. For better compensation two extra coils were wound on the outside of the primary coil (Fig.1 and Table 1). By means of a small electronic circuit, compensation both in phase and in voltage was adjustable (Fig.2). The power supply for the primary coil was provided by an oscillator (1), Hewlett-Packard 299CD and two power amplifiers (2,3), Hewlett-Packard 6824A. The detection part was formed by a lock-in amplifier (7), P.A.R. HR-8 and a recorder (8), Linseis L660/20. A frequency of 270 Hz was used in the system to avoid influences of the 50 Hz mains. In the secondary coil a Dewar vessel or a flow reactor could be inserted. The Dewar was used when static adsorption-desorption measurements were done with the catalyst in a transportable glass cell, a flow reactor was used when magnetization changes of the catalyst during the reaction were measured. Precision of the magnetic system can be expressed as about 1% of full degree of coverage of catalyst NZ 10. Samples of 500 mg NZ 10 were used both in adsorption and reaction experiments. Tests with increasing amounts of Mohrs salt showed the linear relationship between output voltage and sample quantity. Also a linear

TABLE 1

DATA OF THE AC-PERMEAMETER

Coil	Turns	Copper wire diameter (mm)	Current r.m.s. (amp)	Frequency (Hz)	Field strength (Oe)	Length (mm)	Diameter (mm)
Primary	845	1	1	270	56	190	54
Secondary	360	0.2				20	38
Compensation	12	1				12	100

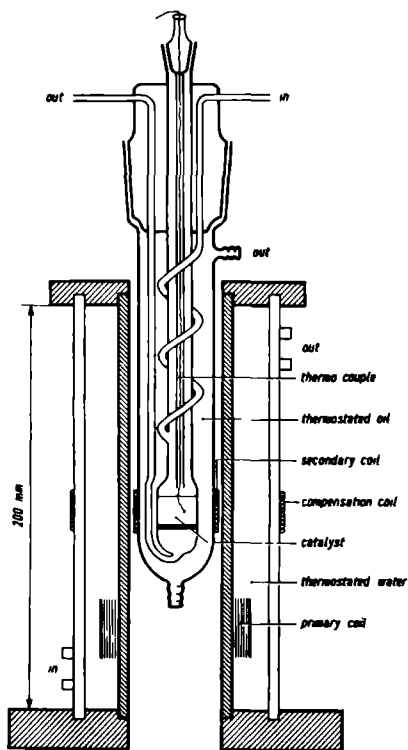


Fig.1. AC-permeameter with glass system for flow experiments. Only one half of the coil system is shown.

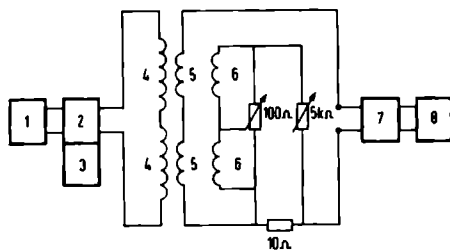


Fig.2. Schematic diagram of the AC-permeameter. (1) oscillator, (2,3) power amplifiers, (4) primary coil, (5) secondary coil, (6) compensation coil, (7) detector, (8) recorder.

relationship existed between the current through the primary coil and the output voltage. In absolute measurements of the magnetization, corrections were made for the diamagnetism of the all glass adsorption cells or glass reactor. The volumetric adsorption system consisted of a glass system with known volume connected with a precision pressure gauge, Texas Instr. model 145-01. For the adsorption of benzene and the other hydrocarbons, greaseless stopcocks were used and glass connections with viton O-ring seals.

Between the admittances of a portion of gas we let two hours pass, after which equilibrium was almost established. The flow reactor contained a porous glass disk of 24 mm diameter on which the catalyst bed was situated, as is shown in Fig.1. Normally the signal of the catalyst in the reactor was compensated, so that changes in the magnetization were measured sensitively. The catalyst was reduced at 450°C during 4 hr with a hydrogen flow of 60 l (STP) hr<sup>-1</sup>. Hydrogen was pumped off at 450°C during 2 hr at a pressure of 10<sup>-4</sup> Torr.

## RESULTS AND DISCUSSION

In the introduction we have seen that the magnetic system in combination with the catalyst must meet several requirements, before we can measure the magnetization at low field strength quantitatively.

In the first place the catalyst must be superparamagnetic over the range of experimental conditions. Since every catalyst has a particle size distribution, it is possible that, even in a catalyst with a small average diameter, large particles occur, which are no longer in thermodynamical equilibrium with the direction of the magnetic field. As a test of the superparamagnetic behaviour we measured the magnetization as a function of  $H/T$ . According to

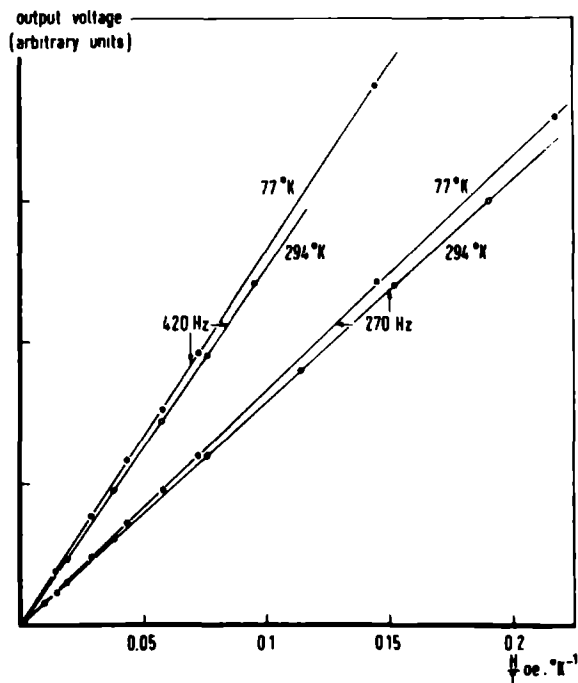


Fig.3. Output voltage (proportional to the magnetization) as a function of  $H/T$  (field strength / absolute temperature) for nickel-silica catalyst NZ 10 at two frequencies of the magnetic field and two temperatures of the catalyst.

the low-field approximation expressed in equation (a),  $M$  vs.  $H/T$  must be linear, after correction for the temperature dependence of the spontaneous magnetization, derived from (15). Figure 3 shows the results for the temperatures 294 and 77°K and the frequencies 270 and 420 Hz. The output signal at 420 Hz is higher than at 270 Hz because the output voltage is proportional to the frequency. If not all particles behave superparamagnetically, one expects a lower signal at lower temperature. However, the reverse is the case. Selwood (4) has mentioned this effect already. A lowering of the Curie temperature of the metal by 70°C could account for the difference in his results. If we base the correction in the spontaneous magnetization on a Curie temperature 80°C lower than of bulk nickel, the lines which represent the relationship between the output voltage and  $H/T$ , shown in Fig.3, coincide at both frequencies.

The effect of the temperature on the magnetization is shown in Fig.4. For



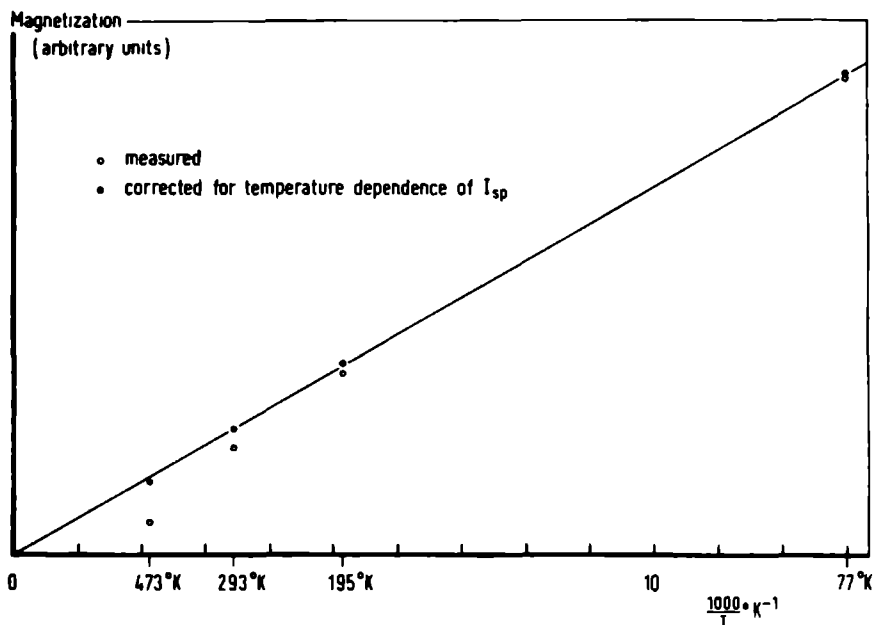


Fig.4. Magnetization as a function of  $1/T$  ( $1/\text{absolute temperature}$ ) for nickel-silica catalyst NZ 10.

the correction of the temperature dependence of the spontaneous magnetization a Curie temperature of  $551^\circ\text{K}$  was used. A straight line through the origin is obtained, indicating that the catalyst NZ 10 behaves completely superparamagnetically in a magnetic field of 56 Oe at 270 Hz from  $77^\circ\text{K}$  to higher temperatures, and indicating that the low field approximation is valid under these conditions.

#### *Magnetization-Volume Isotherms for Hydrogen Adsorption*

To a sample of nickel-silica catalyst NZ 10 reduced and evacuated at  $450^\circ\text{C}$ , hydrogen was admitted in small portions at  $20^\circ\text{C}$ . Each time a new volume of hydrogen was admitted, the magnetization strongly decreased at first, then increased slightly due to the dissipation of the heat of adsorption. Within 30 min this temperature effect vanished, but after this a slower increase occurred for the portions in the first half of the isotherm. The resulting magnetization volume isotherm is given in Fig.5. The fractional change of magnetization amounted to 48.5% after adsorption of 76 ml  $\text{H}_2$  STP/ g Ni-metal. The broken lines in the figure indicate that, instead of two hours, we let a whole night pass

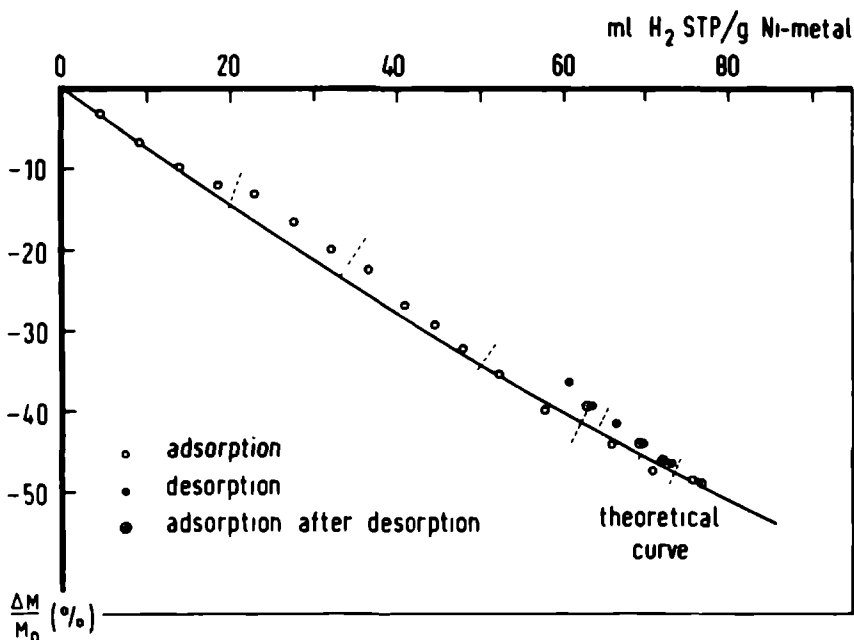


Fig.5. Magnetization-volume isotherm for hydrogen ad- and desorption on nickel-silica catalyst NZ 10 at 20°C. The broken lines indicate a time lapse of 16 hr.

before a new gas admission. The irregular course of the isotherm is rather striking; especially after the first night a step can be seen in the isotherm. This effect was reproducible with other samples.

In order to compare experimental MV-isotherms with a suitable theoretical isotherm for this catalyst, an expression for the particle size distribution of nickel in the catalyst has to be found. Since only three expressions can be formulated from which such a measure for the distribution can be derived, it can involve three adjustable parameters at most, so that the distribution over only three nickel crystallite sizes may be calculated. From the hydrogen adsorption we found an average particle diameter  $D_{H_2}$  of 15.1 Å (1,16). A comparison with the magnetization of Mohr's salt made it possible to determine the volume susceptibility of catalyst NZ 10, 0.030, from which we calculated an average diameter  $D_X$  according to Wösten et al.(9), amounting to 25.9 Å. Since  $D_{H_2}$  is chiefly determined by the small particles and  $D_X$  by the large particles, a distribution over the sizes 10, 20 and 30 Å will be fairly realistic. In the appendix the derivation of the equation for the theoretical magnetization-vo-

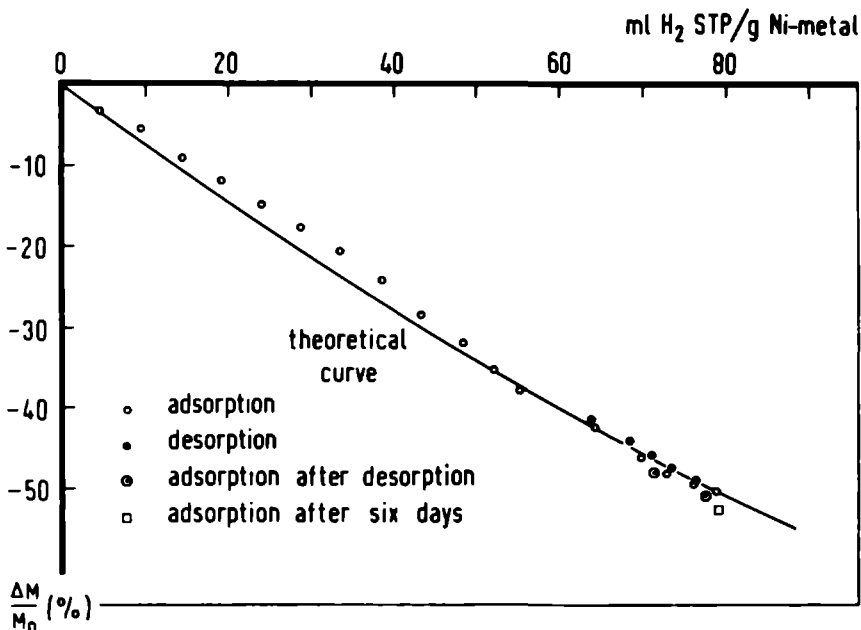


Fig.6. Magnetization-volume isotherm for hydrogen ad- and desorption on nickel-silica catalyst NZ 10 at 20°C. The equilibrium time of each measuring point was 24 hr.

lume isotherm is given. A homogeneous distribution of hydrogen over the crystallites was assumed.

In Fig.5 the desorption branch of the isotherm does not coincide with the adsorption branch. This effect will be discussed later.

In Fig.6 a MV-isotherm is shown, in which an equilibration time of one day was used. The experimental isotherm exhibits a more regular course than the isotherm shown in Fig.5. The slope for an adsorbed quantity of 50 ml is steeper than at small amounts adsorbed. Adsorption and desorption almost coincide. The experimental and theoretical MV-isotherm meet for hydrogen pressures above 1 Torr.

How can we explain the deviation of the experimental isotherm from the theoretical isotherm ?

If hydrogen adsorbed initially in the outer shell of the catalyst pellet (indicating a high sticking probability) and would move to the interior of the pellet by slow diffusion / migration, the magnetization should further decrease with time instead of increase, as a consequence of the square dependence of

the magnetization on the number of metal atoms per crystallite. Therefore a different explanation has to be found.

A spill-over effect by which dissociated hydrogen migrates to the support, might be an explanation for the increase in magnetization after one night. The hydrogen atoms which leave the metal, no longer cause a decrease of magnetization. In order to explain the increase of magnetization during a night several ml of the adsorbed hydrogen have to migrate to the support. For two reasons we reject spill-over as the cause of the observed effect. Firstly, on silica, spill-over is not firmly established and secondly, silica lacks sufficient adsorption power, required for this fairly large amount of dissociated hydrogen. (By evacuation at 450°C water molecules are and hydrogen molecules are not split off by the silica.)

A more probable explanation is the gasphase transition of hydrogen from large to smaller crystallites, the heat of adsorption being assumed to be larger on the smaller crystallites. In the first part of the MV-isotherm the distribution of admitted hydrogen over the crystallites may be assumed to be homogeneous. This is indicated by the fact that the theoretical isotherm there coincides with the experimental one. During one night the magnetization increased corresponding to a transition of several ml  $H_2$  STP/ g Ni-metal from large to small crystallites. Assuming that the hydrogen adsorption is immobile, with a heat of adsorption of 25 kcal/mol in the first part of the isotherm, a desorption rate may be calculated with transition state theory of about 1 ml  $H_2$  STP/ g Ni-metal per 15 hr, thus in the same order of magnitude as the observed gas phase transition. After about 50 ml  $H_2$  has been added, the gas pressure is 1 Torr and the desorption rate becomes so large (the heat of adsorption at higher degrees of coverage is much smaller than 25 kcal/mol) that a homogeneous distribution of hydrogen is the result : the theoretical and experimental isotherms meet.

At higher temperatures the gasphase transition should proceed at a higher rate. In experiments for isotherms shown in Figs. 7 and 8, after each addition of hydrogen, the sample was placed in an oven at 200°C during 15 min. In Figs. 7 and 8 the deviation from the theoretical curve is much more pronounced than in Fig. 6. Obviously the heat treatment gave the adsorbed hydrogen a better opportunity (by subsequent adsorption and desorption) to attain places with higher heat of adsorption, apparently on the smaller crystallites.

The maximum quantity of hydrogen taken up as appears from the data in Fig. 7, is somewhat smaller than as appears from the data in Fig. 5, because the sample in the experiments from which the results are shown graphically in Fig. 7 was

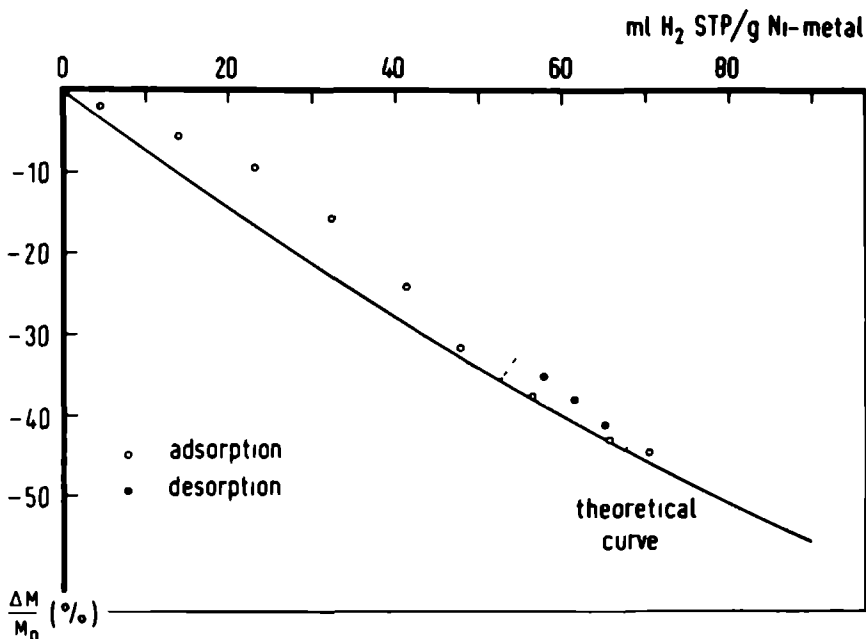


Fig.7. Magnetization-volume isotherm for hydrogen ad- and desorption on nickel-silica catalyst NZ 10 at 20°C. After each ad- and desorption the catalyst sample was held at 200°C for 15 min. The broken lines indicate a time lapse of 16 hr.

three times evacuated at 450°C, which resulted in a slight sintering of the crystallites and a smaller total metal surface area. The sample used for the measurement of the MV-isotherm shown in Fig.8, was evacuated twice at 450°C.

Figure 8 also shows a MV-isotherm for hydrogen adsorption at -80°C. In comparison to the adsorption at 20°C an extra adsorption occurred which did not decrease the magnetization, apparently being physisorbed hydrogen. The desorption branch shows the same effect. At first physisorbed hydrogen is desorbed, the magnetization remaining the same, and after that, chemisorbed hydrogen is desorbed which results in an increase of the magnetization. Here also the desorption branch of the chemisorbed part of the isotherm does not coincide with the adsorption branch. Only at larger quantities desorbed, ad- and desorption isotherms can meet again, as is demonstrated by one desorption point at 20°C. Possibly, at this coverage, hydrogen is more homogeneously distributed over the crystallites after this desorption than after the adsorption procedure with the treatment at 200°C, which was not used after the desorption procedure.

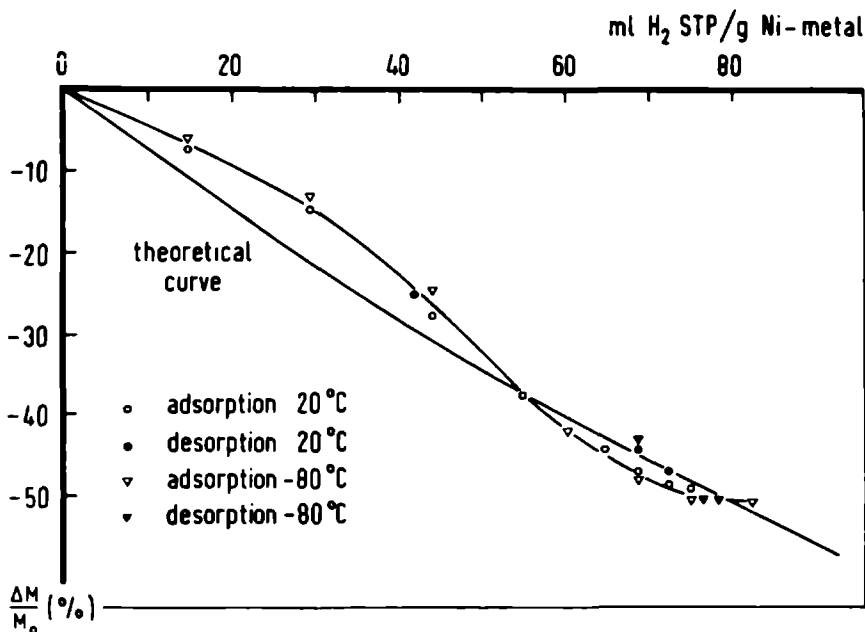


Fig.8. Magnetization-volume isotherm for hydrogen ad- and desorption on nickel-silica catalyst NZ 10 at 20°C and -80°C. Only after each *adsorption* the catalyst sample was held at 200°C for 15 min.

Martin et al.(17) found a hysteresis in saturation magnetization-volume isotherms of hydrogen adsorption and desorption on nickel catalysts, especially on not completely reduced samples. When silica was used as a support for nickel the hysteresis was not as clearly pronounced as on other supports. On  $\text{Ni-}\gamma\text{Al}_2\text{O}_3$  the magnetization even increased as a result of adsorption of hydrogen at 200°C, although the catalyst was completely superparamagnetic. Martin et al. ascribed this effect to the existence of two forms of chemisorbed hydrogen. One form decreased the magnetization in the normal way, the other increased the magnetization after a more activated adsorption. In our experiments the maximum decrease of the magnetization was independent from the time or temperature of hydrogen adsorption. In the case of an activated adsorption, giving rise to a positive change in the magnetization, there should be a difference in the maximum decrease of the magnetization depending on the adsorption time. However, such an effect was not found.

Apart from the normal adsorption form, decreasing magnetization, a slow ad-

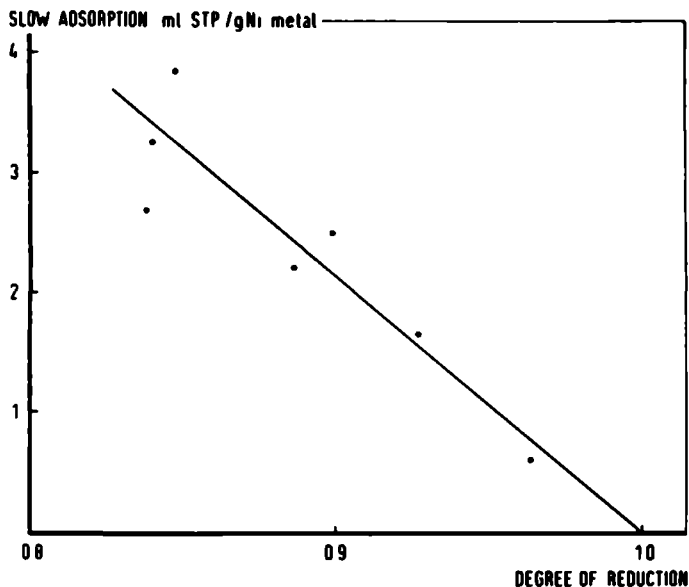


Fig.9. Slow adsorption of hydrogen during one night after measurement of an adsorption isotherm for hydrogen in 8 hr, as a function of the degree of reduction of a series nickel-silica catalysts.

sorption occurred in our experiments. This form was most clearly observable if, in one addition, hydrogen was admitted to the catalyst up to almost full coverage. After one night some more hydrogen was adsorbed and the magnetization was also somewhat decreased. This slow adsorption was measured for Ni-SiO<sub>2</sub> catalysts with different nickel content. It was found that after an adsorption isotherm had been measured in eight hours, the following slow adsorption during one night was inversely proportional to the degree of reduction of the catalyst. The results are shown graphically in Fig.9. Probably the slow adsorption is an activated adsorption on not-reduced nickel. The difference between the adsorption and desorption branch of the MV-isotherm can therefore be attributed to the slow adsorption. This adsorption form does hardly contribute to the magnetization, which points also in the direction of adsorption on non-metallic nickel, e.g. nickelsilicate.

The isotherm for renewed adsorption after a partial desorption coincides with the desorption isotherm, so that, when the catalyst has been covered by hydrogen at 1 atm, changes in coverage relate to the magnetization following the desorption isotherm. To the experiments during the hydrogenation of ben-

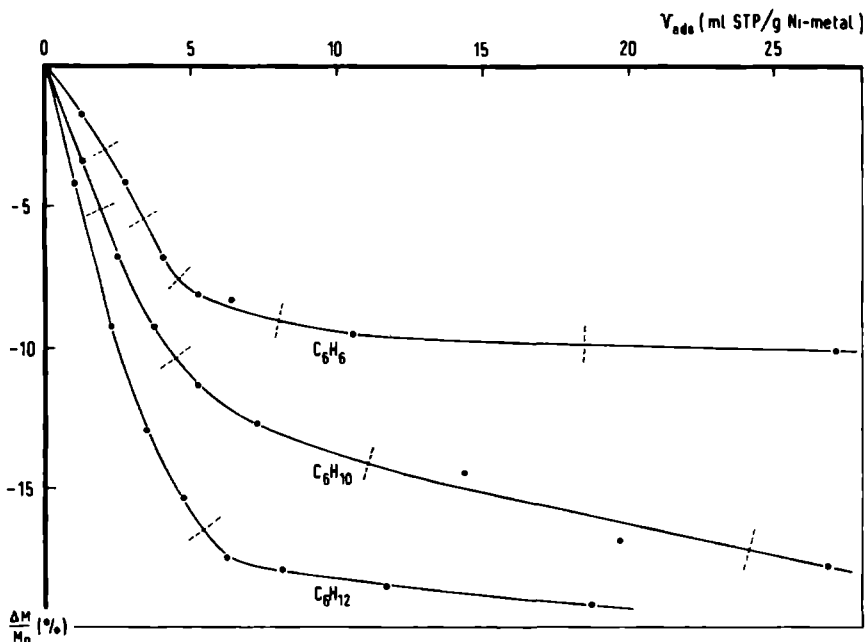


Fig.10. Magnetization-volume isotherms for benzene, cyclohexene and cyclohexane on nickel-silica catalyst NZ 10 at 20°C. The broken lines indicate a time lapse of 16 hr.

zene, we applied the desorption branch of the MV isotherm shown in Fig.8, for the correlation between hydrogen coverage and magnetization.

#### *Magnetization-Volume Isotherm for Benzene Adsorption*

In these experiments we admitted small doses of benzene vapour to a freshly reduced hydrogen-free catalyst (NZ 10) at 20°C. As physical adsorption can occur, we kept the first doses so small that the pressure after adsorption remained below  $10^{-3}$  Torr. A typical isotherm is shown in Fig.10. The maximum relative decrease in magnetization is only -10%, which, in comparison with hydrogen, is rather small. Obviously benzene cannot occupy the whole surface, as was already demonstrated by Selwood (4) and in our own experiments (2).

A scrupulous analysis of the form of the MV-isotherm reveals that the second addition of benzene lies a little above the line between addition one and three. This deviation was measured reproducibly. Apparently, on this catalyst the benzene molecules were not distributed homogeneously, just as Martin et al.



(6) found on their nickel-silica catalyst. The heating procedure, used with hydrogen to make the deviation from the homogeneous distribution more pronounced, was not applicable because at high temperatures benzene dissociates in fragments or even forms carbides (18). The horizontal part of the MV-isotherm indicates that this adsorption has a physical nature. Although the pressure after the last benzene addition was about  $10^{-1}$  Torr, evacuation of the sample to  $10^{-4}$  Torr for 15 min at 20°C did not change the magnetization, evidently only physically adsorbed benzene is removed.

From the ratio of the slopes of the MV-isotherms of hydrogen and benzene a number of bonds may be formally derived. Because of the inhomogeneous adsorption of hydrogen and probably also of benzene, we ought to compare the slopes of those parts of MV-isotherms which represent adsorption on the same crystallites, which is, however, quite impracticable. If we compare the initial slope of the MV-isotherm of benzene with the one for a homogeneous distribution of hydrogen, then the number of bonds is 5.3, whereas this number is 10 if we compare the benzene isotherm with a preferential hydrogen adsorption on the small crystallites. In saturation magnetization measurements Martin et al.(5,18) found that benzene formed 8 bonds with nickel at 25°C. If benzene is somewhat more homogeneously divided over larger and smaller crystallites than hydrogen in the experiments from which the results were shown in Fig.7, the number of bonds may be close to 8.

The other comments on the assignment of a bond number, as mentioned in the introduction, apply more or less. For example, we can hardly believe that spillover can play a part on our nickel-silica catalyst, for reasons mentioned before. About a backdonation of electrons of the metal to the benzene molecule, being  $\pi$ -adsorbed, nothing can be said, because in the magnetic method an overall effect is measured. As benzene adsorbs in different forms (2), another uncertainty is introduced in the assignment of a bond number.

#### *Magnetization-Volume Isotherm for Cyclohexane Adsorption*

In Fig.10 the MV-isotherm for cyclohexane is shown. The relative decrease of magnetization is about 20% at most, twice as much as for benzene at the same amount adsorbed. Cyclohexane physically adsorbed was removable by evacuation without changing the magnetization. Apparently, all chemisorbed species remained on the surface during this process. A range in bond number can be attached to cyclohexane, in the same way as to benzene. Cyclohexane forms 11 to 20 bonds depending on the reference MV-isotherm for hydrogen. If cyclohexane is adsorbed as benzene and six hydrogen atoms, as Shopov et al.(11) concluded from IR-spec-

troscopy measurements and as is indicated by the maximum decrease in the magnetization, the number of bonds should be between  $5.3+6=11.3$  and  $10+6=16$ . This is within the error introduced by the uncertainty about the partition of hydrocarbon molecules over the different nickel crystallites.

#### *Magnetization-Volume Isotherm for Cyclohexene Adsorption*

In Fig.10 also the MV-isotherm of cyclohexene is shown. In this case the maximum relative decrease of the magnetization is slightly less than for cyclohexane, viz. about -18%. The number of bonds derived from the ratio of the slopes is from 7.3 to 13.7, depending on the reference isotherm of hydrogen. As for cyclohexane, it seems possible that cyclohexene adsorbs as benzene and hydrogen atoms, the number of bonds being in this case between  $5.3+4=9.3$  and  $10+4=14$ .

To get an idea of the dissociative nature of cyclohexene adsorption in a different way, we flowed cyclohexene over the catalyst at different temperatures. No benzene or cyclohexane was detected in the effluent by glc analysis, when we flowed cyclohexene with nitrogen over the catalyst at 20°C. At 130°C disproportionation became detectable and with increasing temperature more benzene and less cyclohexane was formed. In the presence of hydrogen, cyclohexane was the only product up to 200°C in agreement with the thermodynamics of cyclohexene hydrogenation, but with small contact times, also benzene could be detected in the products. More benzene was formed at higher temperatures.

Also these last experiments suggest that at higher temperatures cyclohexene will adsorb in the form of benzene and hydrogen. The dissociated hydrogen apparently can migrate to other benzene/cyclohexene molecules and hydrogenate them to cyclohexane. At a low temperature this migration is perhaps too slow and desorption of benzene more difficult. If enough hydrogen is on the surface, immediately hydrogenation to cyclohexane, which desorbs from the surface, occurs.

#### *Chemisorbed Quantities*

From the fact that the magnetization of a sample covered with benzene or cyclohexane remains the same after evacuation to  $10^{-4}$  Torr, one expects a quantity of hydrocarbon (benzene, cyclohexene and cyclohexane) on the surface of about 10 ml/g Ni-metal, corresponding to 708, 744 and 762  $\mu\text{g}/(200 \text{ mg cat})$  for benzene, cyclohexene and cyclohexane respectively. The gravimetric values were 500-700, 760 and 450  $\mu\text{g}/(200 \text{ mg cat})$  on a catalyst partially occupied with hydrogen (2). In the gravimetric experiments it was found that the hydrogen coverage did not influence the amount of chemisorbed benzene, while the amount

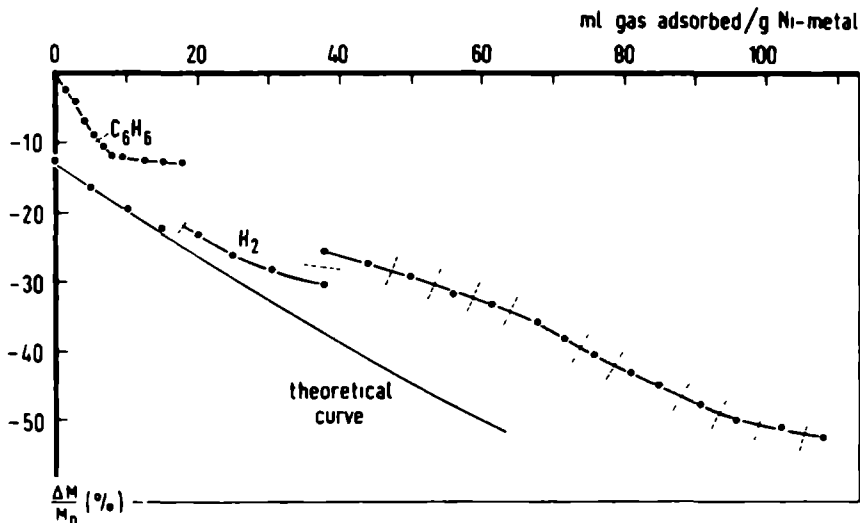


Fig.11. Magnetization-volume isotherm for benzene and for hydrogen over preadsorbed benzene on nickel-silica catalyst NZ 10 at 20°C. The broken lines indicate a time lapse of 16 hr.

of chemisorbed cyclohexane was strongly dependent on hydrogen pressure. Therefore the difference in adsorbed quantities for cyclohexane may be ascribed to the influence of hydrogen coverage.

In another experiment (Fig.11), after measuring a benzene adsorption isotherm and evacuation to  $10^{-4}$  Torr during 90 min, we added hydrogen to the catalyst. Selwood (4) reported that at first hydrogen had to be added to an almost complete coverage before reaction with benzene occurred. As appears from the MV-isotherm shown in Fig.11, hydrogen is at first adsorbed without reaction, but after a few more additions, especially after one night, the steps in the isotherm indicate that reaction took place. The total amount of hydrogen added is 110 ml  $H_2$  STP/g Ni-metal. With the assumption that all the benzene has reacted after several days and that the product cyclohexane is physically adsorbed, we should have added 79 ml  $H_2$ , to cover the nickel surface completely, augmented with about 30 ml hydrogen necessary for reaction with about 10 ml benzene. This summation is in agreement with the experimentally determined quantity.

#### *Magnetization Measurements during the Hydrogenation of Benzene*

Changes in the magnetization of the nickel catalyst could be measured during the flow of different gases. In Fig.12 the successive treatments are given

schematically. The catalyst sample was thermostated at 28°C. Over a clean catalyst successively nitrogen, nitrogen with benzene, hydrogen and hydrogen with benzene were passed. Nitrogen brought about a small decrease in the magnetization, -1 to -2%, benzene -10 to -12% and after hydrogen admission the total decrease in magnetization was the same as for pure hydrogen, -50%. Probably in this case the part of benzene adsorbed in a non-reactive form cannot deny access of hydrogen to that part of the surface, in contrast with the findings of Shopov et al.(11).

Next a flow of pure hydrogen was led over the catalyst. A decrease in the hydrogen pressure from 600 to 75 Torr caused a desorption of about 4 ml H<sub>2</sub> STP/ g Ni-metal. By a pressure decrease to 10<sup>-2</sup> Torr the magnetization increased further as shown in Fig.12. Only a small part of the adsorbed hydrogen desorbed.

After a flow of hydrogen at 600 Torr, a flow of hydrogen with benzene (600 and 70 Torr resp.) caused a further small decrease of the magnetization. Apparently, the surface was not fully covered at 600 Torr hydrogen pressure. A reaction rate  $r_1$  was measured under these conditions. If we decreased the hydrogen pressure to 75 Torr, the magnetization increased corresponding to 4 ml H<sub>2</sub> STP/ g Ni-metal desorbed from the nickel surface. The rate of reaction  $r_2$  was a factor 3 smaller than  $r_1$ . Since the benzene coverage is the same in reactions 1 and 2, as we could conclude from our gravimetric measurements (2) in which the benzene coverage was independent on the hydrogen coverage, a decrease of the degree of occupation by hydrogen ( $\theta_H$ ) with 4 ml influences the reaction rate with a factor 3. If the rate determining step in the benzene hydrogenation is proportional to the first power of  $\theta_H$ , the amount of hydrogen active in the hydrogenation is 6 resp. 2 ml H<sub>2</sub> STP/g Ni-metal at hydrogen pressures 600 and 75 Torr. This hydrogen is only weakly bound, because it is desorbable at 28°C by a pressure decrease from 600 to 75 Torr. This is in agreement with the measurements of Oelderik et al.(19), who found a weak hydrogen adsorption correlating with specific activity for benzene hydrogenation on supported platinum and with, as yet, unreported similar findings in our laboratory on silica supported nickel. The active hydrogen is dissociatively adsorbed, because it decreases the magnetization following the theoretical MV-isotherm, derived for dissociative hydrogen (Fig.8).

After the benzene hydrogenation at a hydrogen pressure of 75 Torr, hydrogen (600 Torr) was passed over the catalyst sample during ½ hr. Next (not further shown in Fig.12) we evacuated the reactor, determined the desorbed volume of hydrogen from the increase of the magnetization (the desorption branch of the

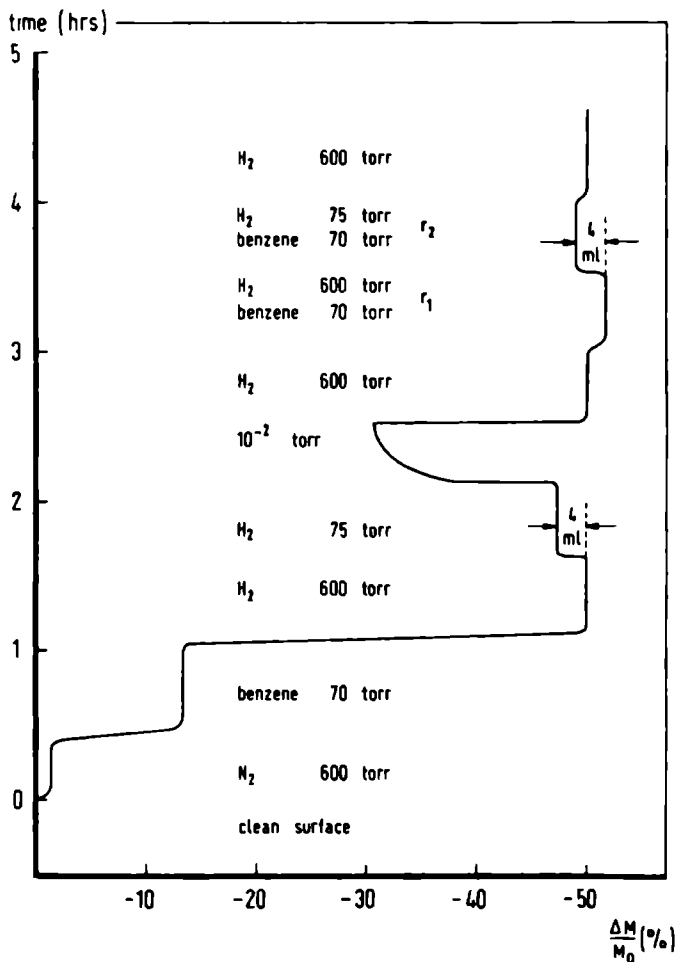


Fig.12. Magnetization changes as a result of the adsorption of nitrogen, benzene over preadsorbed nitrogen, hydrogen over preadsorbed nitrogen and benzene, and during reaction of hydrogen with benzene at different pressures on nickel-silica catalyst NZ 10 at 28°C.

MV-isotherm shown in Fig.8 was used for this purpose), then admitted hydrogen, and from the extra hydrogen taken up by the sample after one night, calculated the quantity of benzene that had remained on the surface. It was known that after a night in hydrogen the remaining benzene had reacted completely (2) and that the resulting cyclohexane was physically adsorbed (2,11). About 3 ml ben-

zene/ g Ni-metal appeared to be inactive with hydrogen during reaction conditions. This is in agreement with our gravimetric experiments (2) on the same nickel catalyst.

About the competition between hydrogen and benzene on the surface of nickel in our catalyst something more can be said. Next to the gravimetric proofs, another indication for the independence of the benzene coverage from the hydrogen coverage can be derived from the following experiment. We evacuated a hydrogen covered sample at 28°C and passed nitrogen with benzene (600 resp. 70 Torr) over the catalyst, now partially covered with hydrogen. No change of the magnetization occurred. However, the quantity of chemisorbed benzene after the flow of nitrogen and benzene was about 10 ml STP/g Ni-metal, as we could derive from the hydrogen adsorption following during one night. This finding is in agreement with a similar gravimetric experiment (2). So benzene was adsorbed on places occupied by hydrogen, which was not desorbed upon evacuation, thus: hydrogen active in the benzene hydrogenation at 28°C does not compete with benzene on the nickel-silica catalyst NZ 10.

#### ACKNOWLEDGEMENT

The authors wish to thank Dr.Ir.J.H.Kaspersma for the helpful discussions and for the measurement of the slow hydrogen adsorption for a series of nickel-silica catalysts.

#### APPENDIX, *Determination of the Particle Size Distribution in Catalyst NZ 10*

With a half sphere model for the nickel particles (16),  $D = \sqrt[3]{\text{volume}}$ , a volume of one nickel atom of  $11 \cdot 10^{-30} \text{ m}^3$  (lattice parameter  $3.524 \text{ \AA}$ ), an average area of one surface nickel atom of  $6.33 \text{ \AA}^2$ , Table 2 gives the number of nickel atoms in the bulk and on the surface of a nickel crystallite. The following three equations determine the partition over the particle sizes 10, 20 and  $30 \text{ \AA}$ :

a) for the total number of nickel atoms per g Ni-metal

$$91 N_1 + 727 N_2 + 2454 N_3 = \frac{1}{58.7} N_{Av}$$

b) for the number of nickel atoms in the surface per g Ni-metal, from the hydrogen adsorption of 79 ml  $\text{H}_2$  STP/g Ni-metal

$$61 N_1 + 243 N_2 + 546 N_3 = 79 \times 2 \times 10^{-3} / 22.4$$

c) for the fractional change of magnetization after 79 ml  $\text{H}_2$  STP/g Ni-metal adsorbed

$$\frac{\Delta M}{M_0} = \text{eq.}(e) = -0.50$$

TABLE 2

NUMBER OF ATOMS IN THE BULK AND ON THE SURFACE  
OF A NICKEL CRYSTALLITE OF HEMISPHERICAL FORM

Diameter (Å)	Number of atoms	
	per particle	in surface
10	91	61
20	727	234
30	2454	546

The result of the three equations is the following partition

$$N_1(10 \text{ Å}) : N_2(20 \text{ Å}) : N_3(30 \text{ Å}) = 27.9 : 2.83 : 1$$

The theoretical equation for the magnetization-volume isotherm reads for a homogeneous distribution of hydrogen over the crystallites :

$$\frac{\Delta M}{M_0} = -0.762 \times 10^{-2} x + 0.16 \times 10^{-4} x^2$$

The last equation has been used for the theoretical curve in the Figs.5-8.

The curve is less steep than in the case of a uniform particle size. The quotient of initial slopes is 1.6 . Selwood (4) already showed that a particle size distribution can decrease the slope of the isotherm by a factor 1.1 to 1.4 .

#### REFERENCES

1. Van Meerten, R.Z.C., and Coenen, J.W.E., *J. Catal.*, in press.
2. Van Meerten, R.Z.C., Verhaak, A.C.M., and Coenen, J.W.E., to be published.
3. Van Meerten, R.Z.C., and Coenen, J.W.E., to be published.
4. Selwood, P.W., "Adsorption and Collective Paramagnetism." Academic Press, New York, 1962.
5. Martin, G.A., and Imelik, B., *J. Chim. Phys.* 68, 1550 (1971).
6. Martin, G.A., de Montgolfier, P., and Imelik, B., *Surface Sci.* 36, 675 (1973).
7. Geus, J.W., Nobel, A.P.P., and Zwietering, P., *J. Catal.* 1, 8 (1962).
8. Geus, J.W., and Nobel, A.P.P., *J. Catal.* 6, 108 (1966).
9. Wösten, W.J., Osinga, T.J., and Linsen, B.G., in "The Structure and Chemistry of Solid Surfaces", Proc. Int. Materials Symp., 4th, Berkeley 1968 (Somorjai, G.A., Ed.). Wiley and Sons, Inc., New York, 1969.
10. Knappwost, A., and Schwarz, W.H.E., *Z. Phys. Chem. N.F.* 67, 15 (1969).
11. Shopov, D., Palazov, A., and Andreev, A., *Proc. Int. Congr. Catal.*, 4th (Moscow) 1968 1, 388 (1971) (Pap.30).
12. Moyes, R.B., and Wells, P.B., in "Advances in Catalysis" (D.D.Eley, H.Pines, and P.B.Weisz, Eds.), Vol.23, p.121. Academic Press, New York, 1973.
13. Bean, C.P., and Livingstone, J.D., *J. Appl. Phys. Suppl.* 30, 120 S (1959).
14. Morrish, A.H., "The Physical Principles of Magnetism." Wiley J., New York, 1965.
15. Weiss, P., and Forrer, R., *Ann. Physik.* 5, 153 (1926) and 12, 279 (1929).

16. Coenen, J.W.E., van Meerten, R.Z.C., and Rijnten, H.T., *Proc. Int. Congr. Catal.*, 5th (Palm Beach, FL) 1972 1, 671 (1973).
17. Martin, G.A., Ceaphalan, N., de Montgolfier, P., and Imelik, B., *J. Chim. Phys.* 70, 1422 (1973).
18. Martin, G.A., and Imelik, B., *Surface Sci.* 42, 157 (1974).
19. Aben, P.C., van der Eijk, H., and Oelderik, J.M., *Proc. Int. Congr. Catal.*, 5th (Palm Beach, FL) 1972 1, 717 (1973).



Gas Phase Benzene Hydrogenation on a  
Nickel-Silica Catalyst

IV. RATE EQUATIONS AND CURVE FITTING

R.Z.C. van Meerten and J.W.E. Coenen

*Department of Catalysis, Faculteit der Wiskunde en Natuurwetenschappen,  
Universiteit van Nijmegen, Toernooiveld, Nijmegen, The Netherlands*

ABSTRACT

Three mechanisms were suitable to describe the hydrogenation of benzene on a nickel-silica catalyst: a mechanism with a rate determining step, the other hydrogen addition steps being faster; a second mechanism based on the assumption that all hydrogen addition steps have the same rate constant, and a third mechanism with a set of slow steps after an adjustable number of fast addition steps.

With a nonlinear least-squares computer fit program values of parameters for the rate equations were calculated. These values are discussed.

The second mechanism appeared to be the most suitable to describe the hydrogenation of benzene on the nickel-silica catalyst.

INTRODUCTION

In preceding papers we described kinetic data (1), gravimetric experiments (2) and magnetic measurements (3) of the hydrogenation of benzene on a nickel-silica catalyst. In this part we will give a mechanistic description of this reaction.

In the literature, many mechanisms with widely diverging basic assumptions have been proposed for the benzene hydrogenation on nickel catalysts. Several authors (4-9) conclude that addition of a hydrogen molecule (instead of an atom) takes place in the rate determining step, viz. the addition of the first

hydrogen molecule according to (5,6,8), the second molecule according to (7) and the third molecule according to (4,9). Addition of adsorbed hydrogen atoms is assumed by Hartog et al.(10,11), Rooney (12) and Snagovskii et al.(13). Snagovskii and coworkers tried two mechanisms: one with one adjustable rate determining step, the other with a set of slow steps. This last mechanism gave the best fit with the experiments. Competition on the surface of the catalyst between benzene and hydrogen is assumed by some authors (4,7) and denied by others (5,8,10,11,13). Canjar et al.(14) used a mechanism in which benzene reacted from the gas phase. Hydrogen reacts from the gas phase according to Jiracek et al.(5). A maximum in the reaction rate at about 180°C is found by Herbo (8), Germain et al.(7) and Nicolai et al.(15). Nicolai and colleagues ascribed the maximum to poisoning of the catalyst, Germain and coworkers, and Herbo to a decrease in reactant adsorption, but no mechanistic description was given.

The aim of this paper is to show that with different mechanisms a fairly good fit with extensive experimental data can be obtained and that a maximum in the reaction rate as a function of temperature follows from the proposed mechanisms.

#### DERIVATION OF THE RATE EQUATIONS

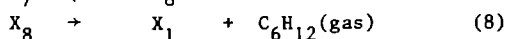
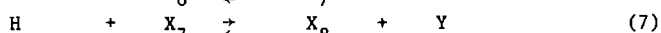
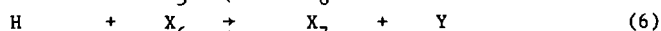
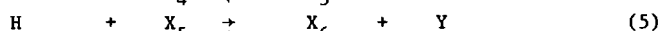
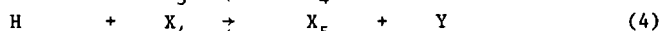
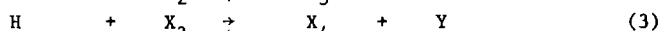
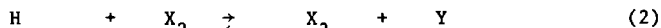
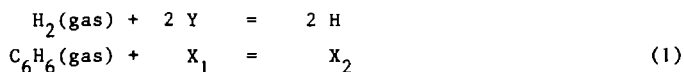
Most mechanisms proposed in the literature fail to produce an order with respect to the hydrogen pressure of 3 at high temperature, decreasing to 0.5 at room temperature, or cannot account for the order with respect to benzene from 0 to 1.0 (1).

For the derivation of rate equations the following was taken into account. Since benzene and hydrogen could be considered non-competitive (2), we assign to hydrogen sites Y and to benzene, together with hydrogenated species, sites X (see list of symbols). As the adsorption of cyclohexane in the presence of hydrogen is very small (2), we assume the concentration of adsorbed cyclohexane to be negligible. The dissociative character of adsorbed hydrogen was amply demonstrated by e.g. Selwood (16) and Martin et al.(17). Our magnetic experiments (3) showed that a weakly bound form of dissociatively adsorbed hydrogen is active in the reaction. Benzene active in the reaction is assumed to adsorb associatively. Adsorbed hydrogen (10,18) and adsorbed benzene (19) are assumed to be in equilibrium with the gas phase.

We further started with the assumption that values for differences in entropy ( $\Delta S$ ) and enthalpy ( $\Delta H$ ) are constant over the entire range of conditions,

although the heterogeneity of the surface may cause the degree of coverage and temperature to have an influence on these parameters. The apparent paradox that a surface which is essentially heterogeneous as a result of surface heterogeneity and induced heterogeneity, behaves (pseudo)-homogeneously in kinetic studies, is discussed in some papers (21-24). In de Bruin's paper (21) a narrow band in the energy distribution appeared to play the active role in the reaction. Therefore we have to consider for the surface reaction one kind of pseudo-homogeneously adsorbed species only. A Langmuir adsorption equation may be applied. In a narrow range of the temperature the active part of the surface may remain the same, but with a large difference in temperature as in our case (20-230°C), it might be possible that the active band shifts. A Langmuir description of the adsorption may still be applied, but with different values of the enthalpy and entropy of adsorption at different temperatures. As will be shown later, we had to assume such a shift in enthalpy of adsorption for benzene and possibly also for hydrogen.

On the basis of these considerations the hydrogenation of benzene may be considered as a sequence of hydrogen atom addition steps.

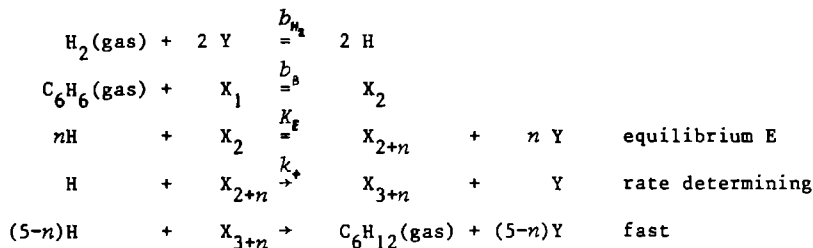


Three possibilities may be distinguished: I. hydrogen addition steps are equilibria up to a rate determining step, further addition steps are faster. II. All addition steps have the same rate constant. III. Like I, except that the additions after the first slow step have the same rate constant as this step.

#### *Mechanism I*

If we assume, according to Snagovskii et al.(13), that the addition of the  $n^{\text{th}}$  hydrogen atom is rate determining and that the foregoing hydrogen addition

steps are in equilibrium, we may write the mechanism as:



The surface coverages are

$$X_2 = b_B p_B X_1$$

$$X_{2+n} = K_E H^n X_2 / Y^n = \exp\{\Delta S_E / R - \Delta H_E / RT\} \times (b_{\text{H}_2} p_{\text{H}_2})^{n/2} X_2 = K_E' p_{\text{H}_2}^{n/2} p_B X_1$$

with  $\Delta S_E$  and  $\Delta H_E$  the entropy and enthalpy differences for equilibrium E. The X surface is assumed to be partly occupied by benzene and  $X_{2+n}$ , so that the following holds:

$$X_1 + X_2 + X_{2+n} = 1$$

The reaction rate becomes

$$r = k_+^H X_{2+n} = k_+ \cdot \frac{(b_{\text{H}_2} p_{\text{H}_2})^{1/2}}{1 + (b_{\text{H}_2} p_{\text{H}_2})^{1/2}} \cdot \frac{K_E' p_{\text{H}_2}^{n/2} p_B}{K_E' p_{\text{H}_2}^{n/2} p_B + b_B p_B + 1}$$

## Mechanism II

Assuming that the rate constants of all hydrogen addition steps to the partially hydrogenated benzene molecule are equal ( $k_{+2} = k_{+3} = k_{+4} = k_{+5} = k_{+6} = k_{+7} = k_+$  and  $k_{-2} = k_{-3} = k_{-4} = k_{-5} = k_{-6} = k_{-7} = k_-$ ) we can treat all intermediates  $X_3$  to  $X_7$  by the steady state approximation. We saw already that  $X_8$  is negligible.

$$X_7 = \frac{A}{A+1} X_6 = \frac{A^2}{A^2+A+1} X_5 = \frac{A^3}{A^3+A^2+A+1} X_4 = \frac{A^4}{A^4+A^3+A^2+A+1} X_3 = \frac{A^5}{A^5+A^4+A^3+A^2+A+1} X_2$$

$$\text{in which } A = \frac{k_+}{k_-} (b_{\text{H}_2} p_{\text{H}_2})^{1/2} \text{ and } X_2 = b_B p_B (1 - X_2 - X_3 - X_4 - X_5 - X_6 - X_7)$$

By substitution we get

$$X_2 = \frac{b_B P_B (A^5 + A^4 + A^3 + A^2 + A + 1)}{b_B P_B (6A^5 + 5A^4 + 4A^3 + 3A^2 + 2A + 1) + (A^5 + A^4 + A^3 + A^2 + A + 1)}$$

$$r = k_{+H} X_7 = k_{+} \frac{(b_{H_2} P_{H_2})^{\frac{1}{2}}}{1 + (b_{H_2} P_{H_2})^{\frac{1}{2}}} \cdot \frac{b_B P_B A^5}{b_B P_B (6A^5 + 5A^4 + 4A^3 + 3A^2 + 2A + 1) + (A^5 + A^4 + A^3 + A^2 + A + 1)}$$

In a different way Snagovskii et al. (15) arrived at about the same expression.

With the steady state treatment, also expressions for the (de)hydrogenation of cyclohexene may be derived. Assuming  $X_2$  and  $X_8$  both zero, the degree of coverage  $X_3$  and  $X_7$  can be expressed in  $X_6$  (adsorbed cyclohexene). The reaction rates of the hydrogenation of cyclohexene to cyclohexane and the dehydrogenation to benzene are respectively:

$$r_{\text{CHE} \rightarrow \text{CHA}} = k_{+H} X_7 = k_{+H} \frac{A}{A+1} X_6$$

$$r_{\text{CHE} \rightarrow \text{B}} = k_{-} X_3 Y = k_{-} \frac{1}{A^3 + A^2 + A + 1} X_6 Y$$

The quotient of these reaction rates, which we measured, is

$$\frac{r_{\text{CHE} \rightarrow \text{CHA}}}{r_{\text{CHE} \rightarrow \text{B}}} = \frac{A^2 (A^3 + A^2 + A + 1)}{(A+1)}$$

At low temperature, when the dehydrogenation does not take place, the reaction rate of cyclohexene hydrogenation may be written:

$$r_{\text{CHE} \rightarrow \text{CHA}} = k_{+H} \frac{b_{\text{CHE}} P_{\text{CHE}} A}{b_{\text{CHE}} P_{\text{CHE}} (2A+1) + (A+1)}$$

### Mechanism III

If the hydrogen addition steps to the adsorbed benzene molecule are equilibria up to  $X_{2+n}$  and further addition steps have the same rate constant, we may consider mechanism III a combination of mechanism I and II. In the derivation of a rate equation,  $X_7$  is expressed in  $X_{2+n}$ , as in mechanism II  $X_7$  was expressed in  $X_2$ .  $X_{2+n}$  is derived following mechanism I, with the difference that now also the degree of coverage of  $X_{3+n}$ ,  $X_{4+n}$  and other intermediates must be taken into account. In this way we may derive for different values of  $n$ :

$n=0$  the same expression as for mechanism II

$$n=1 \quad r = k_+ H A^4 K_E^1 P_{H_2}^{\frac{1}{2}} P_B / \left[ K_E^1 P_{H_2}^{\frac{1}{2}} P_B (5A^4 + 4A^3 + 3A^2 + 2A + 1) + (b_B P_B + 1) (A^4 + A^3 + A^2 + A + 1) \right]$$

$$n=2 \quad r = k_+ H A^3 K_E^1 P_{H_2}^{\frac{1}{2}} P_B / \left[ K_E^1 P_{H_2}^{\frac{1}{2}} P_B (4A^3 + 3A^2 + 2A + 1) + (b_B P_B + 1) (A^3 + A^2 + A + 1) \right]$$

$$n=3 \quad r = k_+ H A^2 K_E^1 P_{H_2}^{\frac{3}{2}} P_B / \left[ K_E^1 P_{H_2}^{\frac{3}{2}} P_B (3A^2 + 2A + 1) + (b_B P_B + 1) (A^2 + A + 1) \right]$$

$$n=4 \quad r = k_+ H A K_E^1 P_{H_2}^{\frac{5}{2}} P_B / \left[ K_E^1 P_{H_2}^{\frac{5}{2}} P_B (2A + 1) + (b_B P_B + 1) (A + 1) \right]$$

$n=5$  the same expression as for mechanism I with  $n=5$

*Rate Constants (k), Equilibrium Constants (K), Adsorption Equilibrium Constants (b) and their Units*

All constants can be split into a temperature dependent and independent part. The surface reaction rate constants can be written as follows from transition state theory :

$$k_+ = n_s \frac{kT}{h} \exp(\Delta S_+^\ddagger / R - \Delta H_+^\ddagger / RT)$$

$$k_- = n_s \frac{kT}{h} \exp(\Delta S_-^\ddagger / R - \Delta H_-^\ddagger / RT)$$

in which  $n_s$  is the number of benzene adsorption sites per square meter. From (3) we know that at room temperature about 1/5 of the nickel metal surface is covered by chemisorbed benzene and from (2), that at 20°C 2/3 of the adsorbed benzene can be eliminated by hydrogenation within  $\frac{1}{2}$  hr. With a surface area of  $41 \text{ \AA}^2$  (2) per benzene molecule, the effective  $n_s$  is at most  $3 \times 10^{17} \text{ sites m}^{-2}$ .  $k_+$  is expressed as the number of benzene molecules converted per second per square meter nickel. To express the reaction rate in  $\mu\text{mol H}_2 \text{ min}^{-1} \text{ m}^{-2}$  as in (1), the multiplication factor  $3 \times 10^{16}$  is introduced.

The activation entropy for the surface reaction refers to a standard state, in which, for localized species (Langmuir approach of adsorption), there is an equipartition of free surface and adsorbed species, viz.

$$\frac{\theta_i}{(1 - \theta_i - \theta_j - \theta_k - \dots)} = 1$$

and in which for mobile species (Volmer approach of adsorption) holds

$$\frac{\theta_j}{(1 - \theta_i - \theta_j - \theta_k - \dots)} = 0.567$$

because for this value of the fraction the  $\theta$  dependence of the molar differential entropy of a Volmer gas disappears (20).

Equilibrium constant  $K_E$  is dimensionless.

The adsorption equilibrium constants for hydrogen and benzene are

$$b_{H_2} = \exp(\Delta S_{H_2}^0/R - \Delta H_{H_2}/RT) \quad \text{atm}^{-1}$$

$$b_B = \exp(\Delta S_B^0/R - \Delta H_B/RT) \quad \text{atm}^{-1}$$

The entropies of adsorption ( $\text{cal mol}^{-1} \text{ } ^\circ\text{K}^{-1}$ ) refer to the standard state  $p = 1 \text{ atm}$ , and the standard states of the adsorbed species are as described above.

#### COMPUTER CURVE FITTING

Since the number of experimental data is large, viz. 260 independent measuring points, describing 19 curves, fitting these data to a reaction rate equation with 8 or 10 parameters appears justified. We substituted the temperature dependence for the constants  $k$ ,  $K$ , and  $b$  in the rate expressions and calculated the parameters for each mechanism by a nonlinear least-squares fit program. The results are given in Table 1.  $F$  denotes the sum of squared differences between experimental and calculated logarithms of reaction rates. For different conditions the relative experimental error proved constant, so that using logarithms in curve fitting, all data receive equal weight.

The final solution arrived at was not always unique: different starting values resulted sometimes in different final values for the parameters. The apparently most reasonable values were then chosen arbitrarily.

With the sets of parameters given in Table 1 it was possible to describe the hydrogenation of benzene on a nickel-silica catalyst satisfactorily. In Figs. 1 and 2 the calculated reaction rates from mechanism II are shown, next to the experimental data.

From the parameter values obtained by fitting, the degrees of occupation by the different surface species  $X_i$  may be calculated. The results are given in Table 2.

#### DISCUSSION

From the  $F$  values in Table 1 it is evident that almost all proposed mecha-

PARAMETERS FOR DIFFERENT MECHANISMS  
ON NICKEL-SILICA  
 $\Delta S$  (cal mol<sup>-1</sup> °K<sup>-1</sup>);

Mechanism	$F^a$	$S.D.^b$	$\Delta S_+^c$	$\Delta H_+^{\ddagger}$	$\Delta S_-^{\ddagger}$	$\Delta H_-^{\ddagger}$
I $n=4$	1.22	17.0	- 9.20	12340		
$n=5$	1.74	20.7	-14.33	12150		
II	0.90	14.5	- 6.00	13766	- 0.08	21149
III $n=1$	0.82	13.8	-10.02	13497	3.77	22928
$n=2$	1.02	15.5	-10.97	13118	- 5.68	19206
$n=3$	0.87	14.2	-15.70	12601	14.30	28471
$n=4$	1.22	17.0	-14.34	12814	- 3.17	20373

<sup>a</sup>  $F$  is the sum of squared differences.

<sup>b</sup>  $S.D.$  is the standard deviation (%).

<sup>c</sup> The number of active sites  $n_s$  was  $3 \times 10^{17}$  sites m<sup>-2</sup> (see text).

nisms are suitable to describe the hydrogenation of benzene on nickel. In Fig. 1 only the calculated values for the reaction rate from mechanism II are shown, but the other mechanisms yield about the same picture. Noteworthy is that a maximum in the reaction rate as a function of temperature, dependent on the hydrogen pressure, is obtained with all mechanisms.

The maximum in mechanism I results from the product of an increasing reaction rate constant  $k_+$  and an, at 180°C ( $p_{H_2} = 600$  Torr), rapidly decreasing degree of coverage of  $X_{2+n}$  (Table 2).

In mechanism II the quantity  $A$  appears to determine the maximum in the same way. At low temperature,  $A$  is much larger than one and the degree of coverage  $X_7$  equals 1/6. At higher temperatures,  $A$  decreases and equals 1, if the reaction rate reaches the maximum value. This means that in the maximum the rate of the backreaction of surface intermediate  $X_{2+n}$  is the same as the rate of the forward reaction of  $X_{2+n}$  with hydrogen:

$$k_+ H X_{2+n} = k_- X_{2+n} Y$$

Beyond the maximum  $A$  is smaller than 1 and again the degree of coverage of  $X_7$  decreases rapidly. In mechanism III the maximum in the reaction rate appears as a result of the rapid decrease of  $X_{2+n}$  and  $X_7$ . Compared to the change in  $X_7$ , the decrease in the degree of coverage of hydrogen has no influence on the appearance of a maximum.

Table 2 shows that the degree of coverage of benzene itself is larger at higher temperature and lower hydrogen pressure. Zlotina et al.(9) also concluded



## NISMS OF BENZENE HYDROGENATION

CATALYST NZ 10

 $\Delta H$  (cal mol<sup>-1</sup>)

$\Delta S_E$	$\Delta H_E$	$\Delta S_{H_2}^0$	$\Delta H_{H_2}$	$\Delta S_B^0$	$\Delta H_B$
- 1.09	-27844	-31.30	-1000	-10.84	- 9367
- 7.00	-28208	-23.74	-1532	-17.04	-11470
		-24.52	-2070	5.35	- 1398
1.43	- 1831	-15.24	-1118	8.04	- 293
-37.23	-23286	-16.00	- 711	44.70	16571
- 7.54	-10473	- 9.91	- 415	19.08	5161
-28.77	-26243	-14.99	-1037	-10.00	- 8277

ed that at 220°C benzene is much more stable on the surface than the other compounds and occupies the major part of the working surface.

The order of reaction with respect to the hydrogen pressure reaches ultimate values of 0.5 and 3.0 in all mechanisms, except in mechanism I with  $n=4$ , where an order 2.5 is the highest possible value. This mechanism is therefore ruled out. The order with respect to the benzene pressure can be zero to 1 in all mechanisms.

Which mechanism is the best one ? Taking into consideration the value of  $F$  only, mechanism III with  $n=1$  should be the best mechanism. But the  $\Delta S$  and  $\Delta H$  are not just empirical parameters, their values should be physically acceptable.

### *Entropies and Enthalpies of Adsorption*

In all mechanisms a very small value is found for the adsorption enthalpy of hydrogen. From the values of the adsorption entropy shown in Table 1 and the standard entropy of gaseous hydrogen 31 e.u., we may deduce that the hydrogen atom on the surface has still 3 to 8 entropy units per gramatom in the standard state. With statistical thermodynamics we calculated that hydrogen adsorbed with two dimensional freedom, has about 5.5 e.u. per gramatom at 25 °C and standard degree of coverage (20), so that  $\Delta S_{H_2}^0$  would be -20 e.u. per mole. The degree of coverage by hydrogen calculated from the fit values of enthalpy and entropy of adsorption is very small, viz. about 0.01 . It must be emphasised that this coverage refers to hydrogen active in the reaction, for which we found already in (3) that it was a small weakly bound part of the total quantity of adsorbed hydrogen.

TABLE 2

COVERAGES OF THE ACTIVE PART OF THE SURFACE  
ACCESSIBLE TO BENZENE, FOR A NUMBER OF MECHANISMS,  
AT DIFFERENT TEMPERATURES AND HYDROGEN PRESSURES <sup>a</sup>

Mechanism	Surface species <sup>b</sup>	Degree of coverage				
		27 °C	135 °C	184 °C	227 °C	227 °C
		$P_{H_2}$ 600 Torr	$P_{H_2}$ 75 Torr	$P_{H_2}$ 600 Torr	$P_{H_2}$ 600 Torr	$P_{H_2}$ 75 Torr
I n=4	$X_1$	0	0.011	0.033	0.157	0.166
	$X_2$	0	0.463	0.404	0.779	0.833
	$X_6$	1.000	0.526	0.563	0.064	0.001
	$X_1$	0	0.016	0.038	0.318	0.357
	$X_2$	0	0.411	0.207	0.580	0.642
	$X_7$	1.000	0.573	0.755	0.102	0.001
	$X_7$					
II	$X_1$	0.016	0.036	0.044	0.094	0.135
	$X_2$	0.164	0.275	0.273	0.512	0.728
	$X_3$	0.164	0.229	0.228	0.228	0.116
	$X_4$	0.164	0.184	0.182	0.101	0.018
	$X_5$	0.164	0.138	0.137	0.043	0.003
	$X_6$	0.164	0.092	0.091	0.017	0.0005
	$X_7$	0.164	0.046	0.045	0.005	0.00006
III n=3	$X_1$	0.0013	0.183	0.045	0.069	0.114
	$X_2$	0.0003	0.429	0.207	0.521	0.860
	$X_3 = X_4$	0	0	0	0	0
	$X_5$	0.333	0.149	0.374	0.329	0.024
	$X_6$	0.333	0.137	0.249	0.069	0.002
	$X_7$	0.333	0.102	0.125	0.012	0.00014
	$X_7$					

<sup>a</sup> catalyst, nickel-silica NZ 10;  $p_B = 70$  Torr.

<sup>b</sup>  $X_1$  = free surface fraction,  $X_2 = (C_6H_6)_{ad}$ ,  $X_3 = (C_6H_7)_{ad}$ ,  $X_4 = (C_6H_8)_{ad}$ ,  
 $X_5 = (C_6H_9)_{ad}$ ,  $X_6 = (C_6H_{10})_{ad}$ ,  $X_7 = (C_6H_{11})_{ad}$ ,  $X_8 = (C_6H_{12})_{ad}$ .

The values found for the enthalpy and entropy of adsorption of benzene for the different mechanisms are not all physically possible. Because we considered the benzene molecule to be adsorbed associatively, a positive entropy and enthalpy of adsorption are impossible. One might, however, assume that the heat of adsorption range of the benzene, converted in the reaction, shifts to higher values at higher temperatures. Accepting this, we can alter the values for the adsorption enthalpy and entropy in such a way, that their changes compensate each other. If we add to the enthalpy of adsorption  $\Delta H_B$  a term  $\alpha T$ :

$$\Delta H'_B = \Delta H_B + \alpha T$$

and add to the entropy this same  $\alpha$ :

TABLE 3  
POSSIBLE CHANGES IN ADSORPTION ENTROPY  
AND ENTHALPY FOR BENZENE ON NICKEL<sup>a</sup>,  
WITHOUT CHANGING THE ADSORPTION EQUILIBRIUM CONSTANT

Mechanism	$\Delta S_B^{ob}$	$\Delta H_B^b$	$\alpha$	$\Delta S_B'^c$	$\Delta H_B'^c$	
					300°K	500°K
I n=5	-17.0	-11470	-10	-27.0	-14470	-16470
			-20	-37.0	-17470	-21470
			-30	-47.0	-20470	-26470
II	5.35	- 1398	-30	-24.65	-10398	-16398
			-40	-34.65	-13398	-21398
			-55	-49.65	-17898	-28898
III n=2	44.7	16571	-80	-35.3	- 7429	-23429
			-90	-45.3	-10429	-28429

<sup>a</sup> nickel-silica catalyst NZ 10.

<sup>b</sup> parameters from Table 1.

<sup>c</sup>  $\Delta S'_B = \Delta S_B^O + \alpha$  ,  $\Delta H'_B = \Delta H_B + \alpha T$  ,  $\Delta S$  in e.u.,  $\Delta H$  in cal mol<sup>-1</sup>.

$$\Delta S'_B = \Delta S_B^O + \alpha$$

then the adsorption equilibrium constant remains unaltered :

$$b_B = \exp\{\Delta S_B^O/R - \Delta H_B/RT\} = \exp\{(\Delta S_B^O + \alpha)/R - (\Delta H_B + \alpha T)/RT\} = \exp\{\Delta S'_B/R - \Delta H'_B/RT\}$$

In Table 3 the values of  $\Delta S'_B$  and  $\Delta H'_B$  are shown for different chosen values of  $\alpha$ . With a constant value of the entropy of adsorption, the enthalpy of adsorption shifts to more negative values at higher temperatures.

In adsorption measurements of benzene on nickel at 0°C, Yu et al.(25) found a heat of adsorption of 25 kcal mol<sup>-1</sup> at very low degree of coverage, decreasing to 8 kcal mol<sup>-1</sup> at the monolayer. With statistical thermodynamics we estimated the entropy of benzene adsorbed on the surface at standard coverage and 25°C (20). For the case of mobile adsorption a value of about 31 e.u. has been found; for the case of localized adsorption about 18 e.u., yielding values for the adsorption entropy of benzene of -33 and -47 e.u. respectively. In Table 3 this last value is accompanied by rather high values of the adsorption enthalpy.

Introduction of a term in the entropy proportional to the enthalpy, following Halsey (27), and a similar term as discussed above in the enthalpy, results in an extra term proportional to  $T^2$  in the real enthalpy of adsorption, because of the requirement that the adsorption equilibrium constants

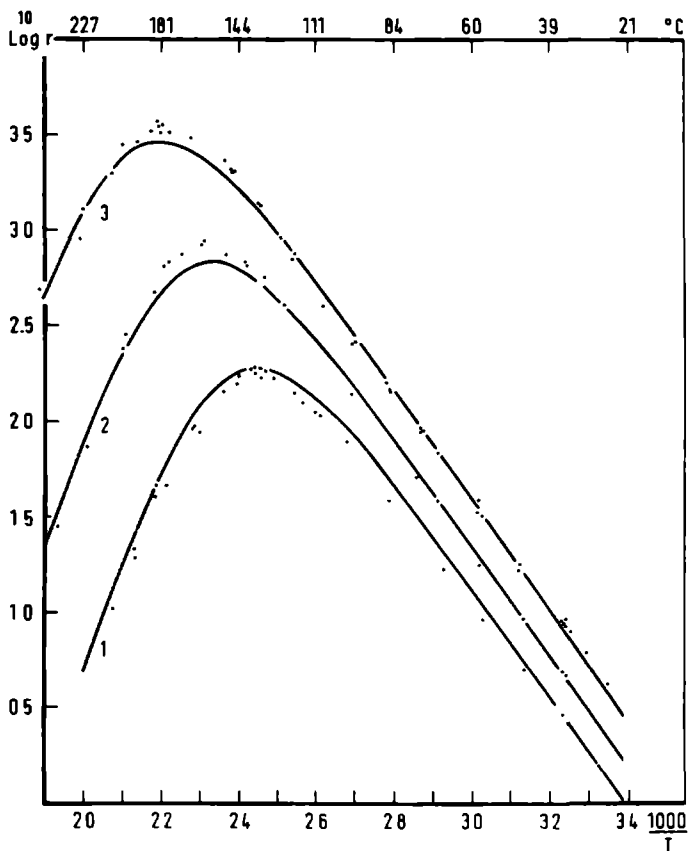


Fig.1. Arrhenius plots showing the effect of temperature and hydrogen partial pressure on the rate of benzene hydrogenation. The dots represent experimental data, the solid curves represent values for the reaction rate calculated on the basis of mechanism II. For the curves indicated by 1, 2, 3 the hydrogen pressures were 75, 200 and 600 Torr respectively; benzene partial pressure, 70 Torr; catalyst NZ 10.

remain the same.

$$\Delta H_B'' = \Delta H_B + \alpha T + \beta T^2 \quad \text{and} \quad \Delta S_B'' = \Delta S_B^0 + \alpha + \beta T$$

It is, however, impracticable to introduce this concept in the computations.

Since also the surface on which hydrogen adsorption occurs, will be heterogeneous, it would be logical to introduce a similar temperature dependence for the adsorption enthalpy of hydrogen. However, the resulting  $\Delta S_{H_2}$  should not be lower than -20 e.u. per mole, so that only for a few of the mechanisms there

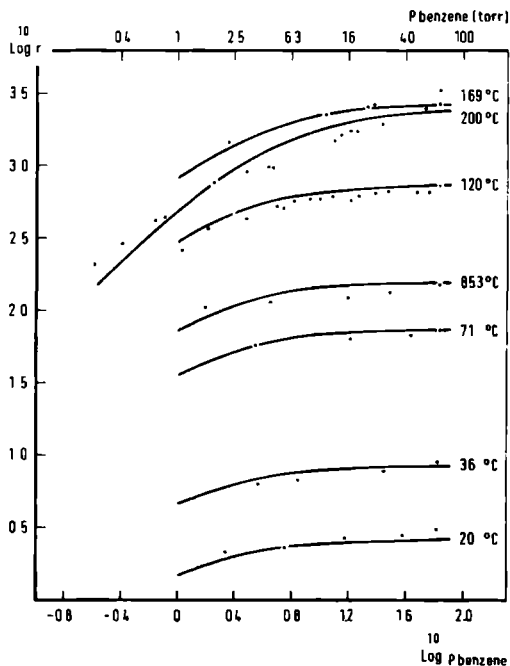


Fig.2. Rate of benzene hydrogenation as a function of benzene partial pressure (Torr). The dots represent experimental data, the solid curves represent values for the reaction rate calculated on the basis of mechanism II. Hydrogen pressure, 600 Torr; catalyst NZ 10.

is a possibility of a significant value of  $\alpha$ . In the extreme case of  $\Delta S_{H_2}^\circ = -9.9$  e.u. (mechanism III,  $n=3$ )  $\Delta S_{H_2}^\ddagger = -20$  e.u. yields

$$\Delta H_{H_2}^\ddagger (500^\circ K) = -415 - 10 \times 500 = -5415 \text{ cal mol}^{-1}$$

$$\Delta H_{H_2}^\ddagger (300^\circ K) = -415 - 10 \times 300 = -3415 \text{ cal mol}^{-1}$$

which is still weakly adsorbed hydrogen.

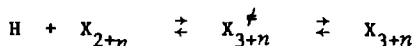
*Activation Entropies of Reaction,  $\Delta S_+^\ddagger$  and  $\Delta S_-^\ddagger$*

We must now consider whether the values of  $\Delta S_+^\ddagger$  and  $\Delta S_-^\ddagger$  are physically acceptable. The result of the computer curve fitting is such, that values for  $\Delta S_+^\ddagger - \Delta S_-^\ddagger$  result. Separate values are then derived by introducing the value for  $n_s$  in the equation for  $k_+$

$$k_+ = n_s \frac{kT}{h} \exp(\Delta S_+^\ddagger / R - \Delta H_+^\ddagger / RT)$$

The value of  $3 \times 10^{17}$  sites  $m^{-2}$  for  $n_s$  derived earlier, represents the total reactive benzene capacity. We should now recall that only part of this capacity is actually reacting at any one temperature, so that the actual  $n_s$  may be much smaller. If the value of  $\Delta S_+^\ddagger$  derived with  $n_s = 3 \times 10^{17}$  is too small, adjustment can be made by reducing  $n_s$ , resulting in a more positive value of  $\Delta S_+^\ddagger$ . For mechanisms II and III  $\Delta S_-^\ddagger$  must be shifted by the same amount as  $\Delta S_+^\ddagger$ , so that the values for  $\Delta S_-^\ddagger$  in Table I are minimum values.

If we accept for instance the scheme which Rooney (12) proposed for the hydrogenation of benzene, the entropy of the surface complex  $X_{2+n}$  will equal approximately the entropy of the surface complex with one more hydrogen atom,  $X_{3+n}$ . The entropy difference  $\Delta S_+^\ddagger - \Delta S_-^\ddagger$  of the reaction



should then be mainly the loss of entropy of an adsorbed hydrogen atom, 4 to 8 e.u. per gramatom. These differences for mechanisms II and III satisfy this condition, with the exception of  $n=1$  and  $n=3$ , so that we discard these mechanisms.

We now consider the separate values for  $\Delta S_+^\ddagger$  and  $\Delta S_-^\ddagger$ . If  $\Delta S_+^\ddagger$  is more negative than -8 e.u., the  $X_{2+n}$  complex loses entropy in going to the activated complex. This, in itself, does not appear impossible, since a bridge with an adsorbed hydrogen atom must be formed, which reduces mobility.  $\Delta S_-^\ddagger$  just represents this difference in mobility, so that positive values for this quantity appear unlikely. This is an added reason to discard mechanisms III  $n=1$  and  $n=3$ .

#### *Activation Enthalpies of Reaction, $\Delta H_+^\ddagger$ and $\Delta H_-^\ddagger$*

About the values of the activation enthalpies of the forward and backward reaction we can only note that their values are about the same in the different mechanisms, so that on this basis no choice can be made.

#### *Entropy and Enthalpy Difference of Equilibrium E, $\Delta S_E$ and $\Delta H_E$*

If the entropy of the adsorbed species  $X_{2+n}$  is about the same as of  $X_{3+n}$ , as we assumed in the foregoing, the entropy difference of the addition of hydrogen atoms in equilibrium E (mech. II and III) will also be determined by the lost entropy of adsorbed hydrogen. In mechanism III  $n=2$  the loss of entropy of two adsorbed hydrogen atoms (-15 e.u.) in equilibrium E cannot cause the value of -37 e.u. for  $\Delta S_E$ . It would imply that the adsorbed benzene molecule

TABLE 4  
CYCLOHEXENE (DE)HYDROGENATION<sup>a</sup>

Temp (°C)	$r_{\text{CHE} \rightarrow \text{CHA}} / r_{\text{CHE} \rightarrow \text{B}}$		
	65 mg cat.	1 mg cat.	calcu- lated <sup>b</sup>
160		3.65	3.63
175	20	2.11	1.35
192	4.26	1.12	0.53
201	2.45	0.79	0.34
215	1.00	0.39	0.19

<sup>a</sup>  $p_{\text{H}_2} = 315$  Torr;  $p_{\text{CHE}} = 67$  Torr.

<sup>b</sup> calculated with the parameters found for mech.II

loses about 22 e.u. in going to  $X_4$ , so that the adsorbed  $X_4$  species has retained  $31 - 22 = 9$  e.u. (assumption  $S_{X_2} = 31$  e.u.). This value is too small even for localized adsorbed X species. Mechanism III  $n=2$  is therefore abandoned.

The enthalpy difference for equilibrium E should more or less reflect the number of hydrogen atom additions, but this trend appears only weakly from the values of  $\Delta H_E$  in Table 1. The mechanisms, retained so far, have about the same value, so that this is not a selection criterion.

Three mechanisms remain with interpretable values of the parameters: mechanism I  $n=5$ , mechanism II, and mechanism III  $n=4$ . On account of the smallest value of  $F$  we prefer mechanism II.

#### *Cyclohexene (De)hydrogenation*

Additional information may be obtained from experiments of cyclohexene disproportionation into benzene and cyclohexane. In Table 4, values are given for the ratio of the rate of hydrogenation to cyclohexane and dehydrogenation to benzene, for two different quantities of catalyst, and as calculated with the parameters found for mechanism II.

According to the thermodynamics of the reaction of cyclohexene with hydrogen, only cyclohexane should be formed. If, however, by using a small quantity of catalyst, the contact time is kept small, the reaction is partly determined kinetically and benzene can desorb from the surface, as was found experimentally. With 1 mg catalyst, the experimental values for the quotient of reaction rates approach already the calculated values, and at still smaller contact times, they may well become identical.

These experiments support mechanism II, because in mechanisms I  $n=5$  and III

$n=4$  the adsorbed species  $X_6$  is in equilibrium with benzene in the gas phase. In a flow system, the benzene gas should be removed and within the assumptions of mechanisms I and III, an equilibrium conversion to benzene must be established. At all temperatures this process is assumed to be rapid, and, accordingly, more benzene than cyclohexene should be formed, also at temperatures below  $180^\circ\text{C}$ . This was not found experimentally, so that also these experiments point to mechanism II as the best description of the hydrogenation of benzene on a nickel-silica catalyst.

An unsolved problem is, that at low temperature the rate of cyclohexene hydrogenation on a nickel surface exceeds the rate of benzene hydrogenation by a factor 1000 (derived from Ref.26). From mechanism II and the expression for the rate of cyclohexene hydrogenation, also derived assuming a set of slow steps, a difference in rate may be calculated of at most a factor 3 (at low temperature  $A$  was much larger than one). Possibly, the number of active sites on a nickel surface is larger for cyclohexene hydrogenation than for benzene hydrogenation, or directly from the gas phase, cyclohexene is adsorbed more reactively than as formed from the hydrogenation of benzene, or a larger part of adsorbed hydrogen is active in the cyclohexene hydrogenation, or, the most probable reason, it is an oversimplification to assume that the rate constants of all hydrogen addition steps in the benzene hydrogenation are equal.

#### ALPHABETIC LIST OF SYMBOLS

$A$	$k_+(b_{\text{H}_2} p_{\text{H}_2})^{1/2} / k_-$ , dimensionless
$b_{\text{B}}$	Adsorption equilibrium constant for benzene, $\text{atm}^{-1}$
$b_{\text{H}_2}$	Adsorption equilibrium constant for hydrogen, $\text{atm}^{-1}$
$F$	Sum of squared differences in computer curve fitting
$H$	Adsorbed hydrogen atom
$\theta$	Degree of coverage by adsorbed hydrogen, dimensionless
$\Delta H_{\text{B}}$	Enthalpy of adsorption for benzene, $\text{cal mol}^{-1}$
$\Delta H_{\text{E}}$	Enthalpy difference for equilibrium E (mech.I,III), $\text{cal mol}^{-1}$
$\Delta H_{\text{H}_2}$	Enthalpy of adsorption for hydrogen, $\text{cal mol}^{-1}$
$\Delta H_{\text{f}}^{\ddagger}$	Activation enthalpy for the forward reaction, $\text{cal mol}^{-1}$
$\Delta H_{\text{b}}^{\ddagger}$	Activation enthalpy for the backward reaction, $\text{cal mol}^{-1}$
$K_{\text{E}}$	Constant for equilibrium E (mech.I,III), dimensionless
$K_{\text{E}}'$	$= K_{\text{E}} b_{\text{B}} (b_{\text{H}_2})^{n/2}$
$k_+$	Reaction rate constant of the forward reaction, $\text{molecules sec}^{-1} \text{ m}^{-2}$
$k_-$	Reaction rate constant of the backward reaction, $\text{molecules sec}^{-1} \text{ m}^{-2}$



$kT/h$	$=0.208 \times 10^{11} T, \text{ sec}^{-1}$
$n$	Number of hydrogen atoms added
$n_s$	Number of benzene adsorption sites per square meter nickel
$p_B$	Partial pressure of benzene, atm
$p_{H_2}$	Partial pressure of hydrogen, atm
$r$	Reaction rate, molecules $\text{sec}^{-1} \text{ m}^{-2}$
$R$	Gas constant, $1.987 \text{ cal mol}^{-1} \text{ }^\circ\text{K}^{-1}$
$\Delta S_B^0$	Entropy of adsorption for benzene, $\text{cal mol}^{-1} \text{ }^\circ\text{K}^{-1} = \text{e.u.}$
$\Delta S_E^0$	Entropy difference for equilibrium E (mech. I, III), e.u.
$\Delta S_{H_2}^0$	Entropy of adsorption for hydrogen, e.u.
$\Delta S_+^\ddagger$	Activation entropy for the forward reaction, e.u.
$\Delta S_-^\ddagger$	Activation entropy for the backward reaction, e.u.
$T$	Absolute temperature, $^\circ\text{K}$
$X_1$	Adsorption site for benzene and hydrogenated species
$X_1$	Free surface fraction of sites $X_1$ , dimensionless
$X_{2+n}$	Adsorbed $C_6H_{6+n}$
$X_{2+n}$	Degree of coverage by $C_6H_{6+n}$ , dimensionless
$Y$	Adsorption site for hydrogen
$Y$	Free surface fraction of sites $Y$ , dimensionless
$\theta$	Degree of coverage, dimensionless

## REFERENCES

1. Van Meerten, R.Z.C., and Coenen, J.W.E., *J. Catal.* in press.
2. Van Meerten, R.Z.C., Verhaak, A.C.M., and Coenen, J.W.E., to be published.
3. Van Meerten, R.Z.C., de Graaf, T.F.M., and Coenen, J.W.E., to be published.
4. Motard, R.L., Burke, R.F., Canjar, L.N., and Beckmann, R.B., *J. Appl. Chem.* 7, 1 (1957).
5. Jiracek, F., Pasek, J., and Horak, J., *Collect. Czech. Chem. Commun.* 33, 3266 (1968).
6. Aben, P.C., Platteeuw, J.C., and Stouthamer, B., *Proc. Int. Congr. Catal.*, 4th (Moscow) 1968 1, 395 (1971) (Pap. 31).
7. Germain, J.E., Maurel, R., Bourgeois, Y., and Sinn, R., *J. Chim. Phys.* 60, 1219, 1227 (1963).
8. Herbo, C., *Bull. Soc. Chim. Belg.* 50, 257 (1941).
9. Zlotina, N.E., and Kiperman, S.L., *Kinet. Catal. (USSR)* 8, 337, 1129 (1967).
10. Hartog, F., Tebben, J.H., and Zwietering, P., *Actes 2ème Congr. Int. Catal.*, (Paris) 1960 1, 1229 (1961).
11. Hartog, F., Tebben, J.H., and Weterings, C.A.M., *Proc. Int. Congr. Catal.*, 3rd (Amsterdam) 1964 2, 1210 (1965).
12. Rooney, J.J., *J. Catal.* 2, 53 (1963).
13. Snagovskii, Y.S., Lyubarskii, G.D., and Ostrovskii, G.M., *Kinet. Catal. (USSR)* 7, 232 (1966).
14. Canjar, L.N., and Manning, F.S., *J. Appl. Chem.* 12, 73 (1962).
15. Nicolai, J., Martin, R., and Jungers, J.C., *Bull. Soc. Chim. Belg.* 57, 555 (1948).

16. Selwood, P.W., "Adsorption and Collective Paramagnetism." Academic Press, New York, 1962.
17. Martin, G.A., de Montgolfier, P., and Imelik, B., *Surface Sci.* 36, 675 (1973).
18. Andreev, A.A., Shopov, D.M., and Kiperman, S.L., *Kinet. Catal. (USSR)* 7, 105 (1966).
19. Zlotina, N.E., and Gudkov, B.S., *Izv. Akad. Nauk SSSR, Ser. Khim.* 9, 1940 (1967).
20. Van Meerten, R.Z.C., Thesis, Nijmegen, 1975. Appendix.
21. De Bruin, H., *Discuss. Faraday Soc.* 8, 69 (1950).
22. Constable, F.H., from "Catalysis" (Emmett, P.H., Ed.), Vol. 1, Ch. 4, Ref. 87. Reinhold Publ. Corp., 1954.
23. Halsey, G.D., *J. Chem. Phys.* 17, 758 (1949).
24. Boudart, M., "Kinetics of Chemical Processes", Ch. 9. Prentice Hall, Englewood Cliffs, N.J., 1968.
25. Yu, Y.F., Chessick, J.J., and Zettlemoyer, A.C., *J. Phys. Chem.* 63, 1626 (1959).
26. Madden, W.F., and Kemball, C., *J. Chem. Soc.* 54, 302 (1961).
27. Halsey, G.D., *Advan. Catal. Relat. Subj.* 4, 259 (1952).

ENTROPIES OF BENZENE AND HYDROGEN  
 ADSORBED ON NICKEL, AND  
 THEIR STANDARD STATES

*Partition Functions*

In statistical thermodynamics the partition function  $Q$  of a particle may be approximated by a product of electronic, translational, rotational and vibrational partition functions.

$$Q = Q_{\text{el}} Q_{\text{trans}} Q_{\text{rot}} Q_{\text{vib}}$$

For a molecule in the gas phase, a volume term  $V$ , and for a molecule with two dimensional freedom, a surface term  $A$  may be segregated from the translational partition function. The zero point energy  $E_0$  may be segregated from the vibrational partition function.

$$Q = Q_{\text{el}} V = Q_{\text{el}} V e^{-E_0/kT}$$

Partition functions are dimensionless. Therefore the dimension of  $Q$  is  $\text{cm}^{-3}$  in the CGS system.

The *electronic* partition function equals 1, if the molecule has no low lying excited state and the ground state is a singlet state.

Per degree of freedom the *translational* partition function is,

$$Q_{\text{trans}} = \left( \frac{2\pi M k T}{N_A h^2} \right)^{\frac{1}{2}} l$$

where  $M$  is the molecular weight,  $N_A$  Avogadro's number,  $l$  in cm.

Per degree of freedom the *rotational* partition function in the rigid rotator approximation is (1),

$$Q_{\text{rot}} = \frac{1}{\sigma} \left( \frac{8\pi^2 I k T}{h^2} \right)^{\frac{1}{2}}$$

Here  $\sigma$  is the symmetry number,  $I$  the moment of inertia of the molecule.

The *vibrational* partition function in the harmonic oscillator approximation is per degree of freedom

$$Q_{\text{vib}} = (1 - e^{-h\nu/kT})^{-1} e^{-E'_0/kT}$$

with  $\nu$  the frequency of vibration and  $E'_0$  the zero point energy for this vibration.

In an *ideal* system of  $N$  indistinguishable particles, the partition function of the system  $Q'$  is expressed in the molecular partition function  $Q$ ,

$$Q' = \frac{Q^N}{N!}$$

or with the Stirling approximation for  $N!$

$$\ln Q' = N (\ln Q - \ln N + 1)$$

Generally one may write for the entropy of a system of  $N$  particles

$$S = k \left[ \ln Q' + T \left( \frac{\partial \ln Q'}{\partial T} \right)_{V,N} \right]$$

The entropy of a system of  $N$  adsorbed particles is

$$S_a = k \left[ \ln Q'_a + T \left( \frac{\partial \ln Q'_a}{\partial T} \right)_{A,N} \right]$$

where  $A$  is the surface area.

#### *Adsorption According to Langmuir*

In the Langmuir approach of adsorption, it is assumed that adsorption is localized, that each site is occupied by one particle, and that the energy of all adsorbed particles is the same (homogeneous surface and no interaction between the particles). The partition function for such a system of distinguishable particles is

$$Q'_a = Q_a^a \frac{N_s!}{N_a! (N_s - N_a)!}$$

The second factor represents the number of ways of distributing  $N_a$  particles on  $N_s$  sites. The molar differential entropy is,

$$\bar{s}_a = N_{Av} \frac{\partial S_a}{\partial N_a} = R \left[ \ln Q_a + \ln \frac{N_s - N_a}{N_a} + T \left( \frac{\partial \ln Q_a}{\partial T} \right)_{N_s, N_a} \right]$$

$$\text{or} \quad \bar{s}_a = R \left[ \ln {}^o Q_a + \ln \frac{1-\theta}{\theta} + T \left( -\frac{\partial \ln {}^o Q_{\text{vib}}}{\partial T} \right) \right]$$

The standard state is defined at  $\theta = 0.5$ , because at this value of  $\theta$  the  $\theta$  dependence disappears. If  $j$  different species are on the surface, the term  $(N_s - N_a)/N_a$  is replaced by  $(N_s - N_a - N_b - N_c - \dots - N_j)/N_a$ . The standard state is now defined at  $\theta_a = 1/(j+1)$ .

#### Adsorption According to Volmer

In the case of an ideal two-dimensional gas with surface per particle  $\sigma_v$  (Volmer gas), the partition function of the system of  $N_a$  particles adsorbed on  $N_s$  sites is,

$$Q'_a = \frac{Q_a^{N_a}}{N_a!} \quad \text{with} \quad Q_a = {}^o Q_a A = {}^o Q_a (N_s - N_a) \sigma_v$$

$$\text{and} \quad \sigma_v = \frac{1 \text{ (cm}^2\text{)}}{N_a (\theta = 1)}$$

$A$  is the free surface area (cm<sup>2</sup>).

The molar differential entropy of this system is

$$\bar{s}_a = N_{Av} \frac{\partial S_a}{\partial N_a} = R \left[ \ln {}^o Q_a + \ln \frac{N_s - N_a}{N_a} + \ln \sigma_v - \frac{N_a}{N_s - N_a} + T \left( -\frac{\partial \ln {}^o Q_a}{\partial T} \right)_{N_s, N_a} \right]$$

$$= R \left[ \ln {}^o Q_a + \ln \frac{1-\theta}{\theta} + \ln \sigma_v - \frac{\theta}{1-\theta} + x + T \left( -\frac{\partial \ln {}^o Q_{\text{vib}}}{\partial T} \right) \right]$$

$x$  arises from the differentiation of  $\ln {}^o Q_a$  to the temperature. With one rotational and two translational degrees of freedom  $x$  equals  $3 \times 0.5 = 1.5$ . The standard state is again defined at the value of  $\theta$ , at which the  $\theta$  dependence of the entropy disappears, i.e. if  $\ln (1-\theta)/\theta = \theta/(1-\theta)$  or if  $\theta = 0.362$ . More generally, the standard state is defined at

$$\frac{\theta_a}{1 - \theta_a - \theta_b - \theta_c - \dots - \theta_j} = 0.567$$

#### ENTROPY OF ADSORBED HYDROGEN ON NICKEL

Hydrogen is adsorbed dissociatively on nickel.

After segregation of the surface term, the partition function for *translation* (2 degrees of freedom) is  $3.28 \times 10^{13} M T \text{ (cm}^{-2}\text{)}$ , where  $M$  is the molecular weight.

TABLE 1  
PARTITION FUNCTIONS FOR HYDROGEN ATOMS ADSORBED ON NICKEL

Partition function	ln Q		$T \frac{\partial \ln Q}{\partial T}$	
	300°K	500°K	300°K	500°K
Translation (2 degrees of freedom)	36.8	37.3	1.0	1.0
Vibration (1 stretch)	0.0	0.003	0.0	0.02
(1 stretch, 2 bending)	0.07	0.28	0.24	0.62

The partition function for *rotation* is irrelevant, because we consider the hydrogen atom.

After segregation of the zero point energy, the expression for the partition function for *vibration* is,

$$Q_{\text{vib}} = (1 - e^{-y})^{-1} \quad \text{with } y = \frac{h\nu}{kT}, \text{ and}$$

$$T \frac{\partial \ln Q_{\text{vib}}}{\partial T} = \frac{y}{e^y - 1}$$

In the literature we could find only one author (2) who reported a stretching frequency for hydrogen adsorbed on nickel. At -60°C this frequency was 1910 cm<sup>-1</sup>. For hydrogen on platinum almost the same value was found (3). Bending frequencies are mostly a factor 0.3 to 0.4 smaller than the frequencies for stretching vibrations. Thence we assigned to hydrogen on nickel one stretching frequency at 2000 cm<sup>-1</sup> and two bending frequencies at 700 cm<sup>-1</sup>.

In Table 1 values are given for ln Q and  $T \frac{\partial \ln Q}{\partial T}$ .

The total entropy of a localized adsorbed hydrogen atom originates only from the entropy of vibration (1 stretching, 2 bending), the atom has no translation

TABLE 2  
ENTROPY OF MOBILE AND LOCALIZED ADSORBED  
HYDROGEN ATOMS ON NICKEL AND OF HYDROGEN IN THE GAS PHASE

Temp (°K)	$\bar{s}_{\text{mobile}}^a$ (cal °K <sup>-1</sup> gatom <sup>-1</sup> )	$\bar{s}_{\text{localized}}^b$ (cal °K <sup>-1</sup> gatom <sup>-1</sup> )	$S_{\text{gas}}^c$ (cal °K <sup>-1</sup> gmol <sup>-1</sup> )
300	5.56	0.62	31.2
500	6.60	1.79	34.8

<sup>a</sup> Standard state  $\theta_{\text{H}} = 0.362$

<sup>b</sup> Standard state  $\theta_{\text{H}} = 0.5$

<sup>c</sup> Standard state  $p_{\text{H}_2} = 1 \text{ atm}$

TABLE 3  
PARTITION FUNCTIONS FOR BENZENE ADSORBED ON NICKEL

Partition function	ln Q		$T \frac{\partial \ln Q}{\partial T}$	
	300°K	500°K	300°K	500°K
Translation (2 degrees of freedom)	41.2	41.7	1.0	1.0
Rotation (axis $\perp$ ring)	2.05	2.31	0.5	0.5
Vibration (1 stretch)	0.85	1.27	0.75	0.84
(1 stretch, 2 bending)	4.33	5.71	2.57	2.72

nor rotation. The total entropy of mobile adsorbed hydrogen atoms is composed of the entropy for translation and vibration (1 stretching). For the surface area of a hydrogen atom on nickel ( $\sigma_v$ ) we used a value of  $6.3 \times 10^{-16} \text{ cm}^2$ . In Table 2 values for the entropies are given.

#### ENTROPY OF BENZENE ADSORBED ON NICKEL

The partition function for *translation* (2 degrees of freedom) is  $3.28 \times 10^{13} M T \text{ (cm}^{-2}\text{)}$ .

If the molecule has one degree of *rotational* freedom, the partition function for rotation is

$$Q_{\text{rot}} = \frac{1}{\sigma} \frac{(8 \pi^2 I_A k T)^{\frac{1}{2}}}{h^2}$$

in which  $I_A$  is the moment of inertia around the sixfold axis perpendicular to the benzene ring,  $29.4 \times 10^{-39} \text{ g cm}^2/\text{molecule}$ . The symmetry number  $\sigma$  is 6.

The partition function for *vibration*. Although no vibrational frequencies for benzene adsorbed on nickel are given in the literature, we may derive an approximate value for the stretching frequency from the stretching vibration of the nickel-hydrogen system. The frequency  $\nu$  of an harmonic oscillator is proportional to the square root of the effective force constant  $k_{\text{eff}}$ , which in turn may be assumed to be proportional to the binding energy  $E$ . With  $\mu$  the reduced mass of the vibrator, we may write

$$\nu = c' \sqrt{(k_{\text{eff}}/\mu)} = c \sqrt{(E_{\text{binding}}/\mu)}$$

The binding energy for two hydrogen atoms is the dissociation energy of a hydrogen molecule added to the heat of adsorption of a hydrogen molecule viz.  $104 + 15 \text{ kcal/mol}$ , yielding a binding energy of about  $60 \text{ kcal/g atom}$ . For associatively adsorbed benzene, the binding energy equals the value of the heat

TABLE 4  
ENTROPY OF MOBILE AND LOCALIZED ADSORBED  
BENZENE ON NICKEL AND OF BENZENE IN THE GAS PHASE

Temp (°K)	$\bar{s}_{\text{mobile}}^a$ (cal °K <sup>-1</sup> gatom <sup>-1</sup> )	$\bar{s}_{\text{localized}}^b$ (cal °K <sup>-1</sup> gatom <sup>-1</sup> )	$S_{\text{gas}}^c$ (cal °K <sup>-1</sup> gmol <sup>-1</sup> )
300	30.9	18.3	64.3
500	42.7	30.7	77.8

<sup>a</sup> Standard state  $\theta_B = 0.362$

<sup>b</sup> Standard state  $\theta_B = 0.5$

<sup>c</sup> Standard state  $p_B = 1$  atm

of adsorption, about 15 kcal/mol. The stretching vibration for the system nickel-benzene then is

$$\nu_{\text{str}} = 2000 \sqrt{\frac{1}{60}} \sqrt{\frac{15}{78}} = 113 \text{ cm}^{-1}$$

From this value the bending frequency is estimated at 40 cm<sup>-1</sup>.

In Table 3 values are given for the partition functions .

Benzene also has internal vibrations, contributing 4.6 e.u. to the entropy of the gas molecule at 300°K, and 14.0 e.u. at 500°K. It was assumed that the adsorbed molecule retained this internal entropy. For the surface area of a benzene molecule the value  $41 \times 10^{-16}$  cm<sup>2</sup> was used. In Table 4 the values for the entropy of adsorbed benzene and benzene in the gas phase are shown.

#### STANDARD STATES FOR THE ENTROPY OF ADSORPTION

The adsorption equilibrium constant  $b$  can be written according to

$$\text{the Langmuir model} \quad b = \exp(\Delta S^0/R - \Delta H/RT) \quad \text{atm}^{-1}$$

$$\text{the Volmer model} \quad b = \exp(\Delta S^0/R - \Delta H/RT - \frac{\theta}{1-\theta}) \quad \text{atm}^{-1}$$

The partition function for an ideal system of  $N$  indistinguishable non-linear gas molecules is  $Q_g' = Q_g^N/N!$ . The molar differential entropy of this system is,

$$\begin{aligned} \bar{s}_g &= R \left[ \ln {}^0Q_g - \ln \frac{N}{V} + T \left( \frac{\partial \ln {}^0Q_g}{\partial T} \right)_{V,N} \right] \\ &= R \left[ \ln {}^0Q_g - \ln p + \ln kT + 3 + T \frac{\partial \ln {}^0Q_{\text{vib}}}{\partial T} \right] \end{aligned}$$

The standard state may be defined at  $p = 1$  atm, consequently  ${}^0Q_g$  is expressed in liter<sup>-1</sup> and  $kT$  in liter atm.



The entropy of adsorption in the adsorption equilibrium constant is a standard entropy,  $\Delta S^0$ ,

$$\Delta S^0 = \bar{s}_a^0 - \bar{s}_g^0$$

In the rate equations of chapter IV we expressed the pressures in atmospheres. Therefore  $\Delta S^0$  in these equations refers to the transition of a mole at 1 atm to the adsorbed state at standard condition:

in the Langmuir approach  $\theta = 0.5$ , or, if also other molecules are on the surface,  $\theta = 1/(j+1)$

in the Volmer approach  $\theta = 0.362$ , or more generally if

$$\frac{\theta_a}{1 - \theta_a - \theta_b - \dots - \theta_j} = 0.567$$

#### REFERENCES

1. Rushbrooke, G.S., "Introduction to Statistical Mechanics." Oxford, at the Clarendon Press, 1949.
2. Kavtaradze, N.N., and Sokolova, N.P., *Russ. J. Phys. Chem.* 44, 1485 (1970).
3. Pliskin, W.A., and Eischens, R.P., *Z. Phys. Chem. N.F.* 24, 11 (1960).

We studied the hydrogenation of benzene on a nickel-silica catalyst (NZ 10) with three different experimental techniques: kinetics (Chapter I), gravimetry (Chapter II) and magnetization measurements (Chapter III). On the basis of the experimental data a number of reaction mechanisms was derived and tested (Chapter IV). With statistical thermodynamics we estimated the entropy of benzene and hydrogen adsorbed on the metal surface (Appendix). The estimated values were compared with values obtained from computer curve fitting.

In Chapter I is described, how in a differential flow reactor the rate of benzene hydrogenation is measured as a function of temperature and partial pressures of hydrogen, benzene and cyclohexane.

The order of reaction with respect to hydrogen rises from 0.5 at 25°C to 2-3 at 200°C. The order of reaction with respect to benzene rises from about 0.1 at 25°C to 0.3-0.5 at 200°C. No inhibition of cyclohexane can be detected. Most striking is that a maximum appears in the reaction rate at higher temperature. Depending on the hydrogen pressure (75-600 Torr) the temperature of the maximum shifts from 135°C to 180°C. Neither poisoning, nor diffusion limitation, nor approach to equilibrium can account for the maximum. It is, however, possible to describe the maximum kinetically, as will be explained in Chapter IV.

With a very sensitive electro-balance we studied the adsorption and reactivity of benzene on our catalyst at different degrees of coverage by hydrogen (Chapter II). The experiments suggest three forms of chemisorption by benzene, covering only part of the surface: a) a reactive form, being the active form in normal benzene hydrogenation, in our experiments discernable up to 110°C, b) a form of low reactivity, not contributing to normal benzene hydrogenation, removable by several hours hydrogen flow at the temperature of adsorption, c) a dissociatively adsorbed form, occurring at high temperature (above 120°C) only if hydrogen is not present during the adsorption of benzene. This last form acts as a poison for the hydrogenation reaction and is removed by hydrogen at 400°C only.

At low temperature the degree of coverage by chemisorbed benzene is independent of the hydrogen pressure (0 - 1 atm) during adsorption of benzene and reaction: benzene has its "own" surface, from which it can desorb hydrogen.

Physical adsorption of benzene was measured as a function of temperature and

benzene pressure.

Adsorbed in hydrogen atmosphere at temperatures from 30 up to 200°C, cyclohexane appears to be easily removable by hydrogen. This is the reason why cyclohexane does not act as an inhibitor in the hydrogenation of benzene.

In Chapter III a simple coil system (AC-permeameter) is described with which we measured the magnetization of the superparamagnetic nickel crystallites in catalyst NZ 10 as a function of the degree of coverage by hydrogen, benzene, cyclohexene and cyclohexane.

Hydrogen is preferentially adsorbed on the smallest crystallites. The hydrocarbons occupy the nickel surface only partially. Only a range in the number of bonds between the hydrocarbon and nickel can be assigned. By evacuation to  $10^{-4}$  Torr, physically adsorbed benzene and cyclohexane can be desorbed, chemisorbed species remain on the surface.

Magnetization measurements during the hydrogenation of benzene show that only a small part of the nickel surface plays a part in the reaction, and that a weakly bound form of dissociatively adsorbed hydrogen is active in the reaction.

In Chapter IV we use the experimental data, described in the foregoing chapters, to propose three reaction mechanisms for the hydrogenation of benzene on nickel: a mechanism (I) with a rate determining step, the other hydrogen addition steps being faster; a second mechanism (II) based on the assumption that all hydrogen addition steps have the same rate constant, and a third mechanism (III) with a set of slow steps after an adjustable number of fast addition steps.

With a least-squares nonlinear computer fit program, values of parameters for the rate equations were calculated. These values are discussed. Entropies of adsorbed species are compared with values estimated with statistical thermodynamics (Appendix).

The second mechanism appears to be the most suitable to describe the hydrogenation of benzene on a nickel-silica catalyst.

In the Appendix, we further pay attention to standard states for entropies of adsorption and of adsorbed particles.

Ter bestudering van de benzeen hydrogenering op de nikkel-silica katalysator (codenaam NZ 10) werden door ons drie verschillende experimentele technieken gebruikt: kinetiek (hoofdstuk I), gravimetrie (hoofdstuk II) en magnetische metingen (hoofdstuk III). Op basis van de experimenteel verkregen gegevens werden drie reaktiemechanismen opgesteld en uitgeprobeerd (hoofdstuk IV). Waarden voor adsorptie-entropieën konden vergeleken worden met statistisch thermodynamisch berekende waarden (appendix).

In hoofdstuk I wordt beschreven hoe in een differentiële flow reactor de reactiesnelheid van de hydrogenering van benzeen wordt gemeten als functie van de temperatuur en partiaaldrukken van waterstof, benzeen en cyclohexaan.

De orde van de reactie in waterstof verloopt van 0.5 bij 25°C tot 2-3 bij 200°C, de orde in benzeen van 0.1 bij 25°C tot 0.3-0.5 bij 200°C, de orde in cyclohexaan is nul over het temperatuurinterval 25-200°C. Opvallend is het optreden van een maximum in de reactiesnelheid bij hogere temperatuur. Afhankelijk van de waterstofdruk (75-600 Torr) verschuift het maximum van 135 naar 180°C. Het maximum kan niet verklaard worden met een vergiftiging van de katalysator, noch met diffusie limitering van reactanten in de poriën van de katalysator, noch met het bereiken van de evenwichtsconversie. Het maximum kan kinetisch verklaard worden, zoals in hoofdstuk IV zal blijken.

Met behulp van een zeer gevoelige balans werd het adsorptieve en reactieve gedrag van benzeen op de katalysator bestudeerd (hoofdstuk II). Drie vormen van adsorptie werden gevonden, die geen van allen het oppervlak geheel bedekten: a) een reactieve vorm die voor een groot deel de actieve vorm is in de normale benzeen hydrogenering; deze vorm is in onze experimenten aantoonbaar tot 110°C, b) een vorm van lage reactiviteit, die niet bijdraagt tot de normale benzeen hydrogenering, c) een dissociatief geadsorbeerde vorm, die bij hoge temperatuur (boven 120°C) optreedt indien tijdens de adsorptie geen waterstof aanwezig is. Deze laatste vorm vergiftigt het oppervlak voor de hydrogeneringsreactie gedeeltelijk, en kan slechts bij 400°C in een waterstof-flow van het katalysator oppervlak verwijderd worden.

Onafhankelijk van de waterstofdruk (0-1 atm) wordt benzeen bij lage temperatuur in gelijke hoeveelheden op de katalysator gechemisorbeerd: benzeen heeft zijn "eigen" oppervlak, waarvan het waterstof kan verdringen.

Naast chemisorptie van benzeen treedt bij lage temperatuur in aanzienlijke mate fysisorptie op.

Indien cyclohexaan geadsorbeerd wordt op de katalysator bezet met waterstof, is het zeer gemakkelijk desorbeerbaar. Dit is de reden waarom cyclohexaan niet remmend werkt (orde nul) op de hydrogenering van benzeen.

In hoofdstuk III wordt beschreven hoe we met een eenvoudig spoelensysteem (AC-permeameter) de magnetisatie van de superparamagnetische nikkel kristallieten in de katalysator NZ 10 gemeten hebben als functie van de bezetting van het oppervlak door waterstof, benzeen, cyclohexeen en cyclohexaan.

Waterstof blijkt bij voorkeur op de kleinste kristallieten geadsorbeerd te worden. De genoemde koolwaterstoffen kunnen het oppervlak slechts gedeeltelijk bezetten, met een aantal banden per molecuul, dat voor benzeen tussen de 5 en 10 ligt en voor cyclohexaan tussen 11 en 20, afhankelijk van de referentie magnetisatie-volume isotherm voor waterstof. De gechemisorbeerde koolwaterstoffen worden bij een druk van  $10^{-4}$  Torr niet gedesorbeerd.

Magnetisatie metingen tijdens de hydrogeneringsreactie tonen aan dat een zwak gebonden vorm van dissociatief geadsorbeerde waterstof actief is in de reactie, die plaatsvindt op slechts een klein deel van het nikkel oppervlak.

In hoofdstuk IV zijn de gegevens uit de in de voorgaande hoofdstukken beschreven experimenten gebruikt voor het opstellen van drie reactiemechanismen en snelheidsvergelijkingen voor de hydrogenering van benzeen op nikkel: een mechanisme (I) met een snelheidsbepalende stap, waarbij de andere waterstof addities sneller verlopen; een tweede mechanisme (II) gegrond op de aanname dat alle waterstof addities dezelfde snelheidsconstante hebben, en een derde mechanisme (III) met een serie langzame stappen na een aantal snelle addities.

Met een kleinste-kwadraten niet-lineair computer fit programma werden waarden berekend voor parameters in de reactiesnelheidsvergelijkingen. De waarden van de entropie parameters worden vergeleken met statistisch thermodynamisch geschatte waarden van entropieën voor geadsorbeerde waterstof en benzeen (appendix)

Het tweede mechanisme blijkt het meest geschikt om de hydrogenering van benzeen op de nikkel-silica katalysator NZ 10 te beschrijven.

In de appendix wordt verder aandacht besteed aan de standaardtoestanden, zoals die gelden voor de entropie van geadsorbeerde deeltjes en voor het entropieverschil van het adsorptieproces.

I

Dat de snelheid van waterstof-deuterium uitwisseling in benzeen op nikkel geen maximum vertoont als functie van de temperatuur, in tegenstelling tot de hydrogenering van benzeen, is toe te schrijven aan een ten naaste bij gelijk blijvende bezettingsgraad van benzeen.

Zlotina, N.E., and Gudkov, B.S., *Izv. Akad. Nauk SSSR, Ser. Khim.* 9, 1940 (1967).  
Dit proefschrift, blz. 60.

II

In de reacties van skelet-isomerisatie, cyclisatie en hydrogenolyse van n-hexaan op ultra dunne en dikkere nikkel en platina films, schrijven Anderson et al. de verhoogde selectiviteit voor de vorming van C<sub>6</sub>-produkten op ultra dunne films toe aan de relatief grotere fractie laag gecoördineerde metaal-atomen op hoeken van de zeer kleine (<20 Å) kristallieten waaruit de films bestaan. Een dergelijk effect van kristallietgrootte verklaart de geringe mate waarin de hydrogenolyse plaatsvindt op de nikkel-silica katalysator NZ 10 met kristallieten van 10 tot 30 Å tijdens de hydrogenering van benzeen.

Anderson, J.R., McDonald, R.J., and Shimoyama, Y., *J. Catal.* 20, 147 (1971).  
Dit proefschrift, blz. 10.

III

Het aantal active sites voor benzeen hydrogenering op nikkel wordt door Evzerikhin op  $1.5 \times 10^{19} \text{ m}^{-2}$  gesteld. Dit aantal is veel te hoog, een reden waarom de door hem berekende transmissiecoëfficiënt te klein is.

Evzerikhin, E.I., *Russ. J. Phys. Chem.* 40, 890 (1966).

IV

Indien één van de reactanten in een reactie in meetbare mate fysisch geadsorbeerd wordt aan het oppervlak van een poreuze katalysator, kan men de temperatuur van de katalysator afleiden uit de mate van fysische adsorptie van die reactant.

Dit proefschrift, blz. 20.

V

Het is noodzakelijk bij het gebruik van entropieën of entropieverschillen de bijbehorende standaardtoestand(en) te vermelden.

## VI

De methoden ter analyse van concentratiecurven van expiratiegassen van mensen, zoals ontwikkeld door van Meerten, zijn eveneens toepasbaar op die van dieren, en hebben ook daar diagnostische waarde.

Van Meerten, R.J., Proefschrift, Nijmegen, 1966.

## VII

Het is tegenstrijdig, dat belanghebbenden volgens artikel 29 van de Wet op de Ruimtelijke Ordening tot aan de Kroon toe bezwaren tegen een bestemmingsplan kunnen indienen, terwijl hun de toegang tot de Kroon ontnomen wordt door de toepassing van artikel 11 van de Wet op de Ruimtelijke Ordening, tenzij zij tegen de toepassing van artikel 11 een bezwaar indienen.

## VIII

De kleuren van stippen die gebruikt worden ter bewijzing van wandelpaden in bos en op veld, zouden zodanig moeten zijn, dat overal in Nederland een bepaalde kleur dezelfde afstand aangeeft.

## IX

Ter verkrijging van een duurzaam bomenbestand langs wegen, dient er naar gestreefd te worden, dat jonge, middelmatig oude en oude bomen in gelijke mate vertegenwoordigd zijn.

De Honderd Ouden van de Groesbeekseweg, 1972

## X

Gelet op de door de regenperiode ontstane kwaliteitsverschillen tussen Bordeaux wijnen van de oogst 1974, zou de wijnruver gebaat zijn bij een meteorologische voorspelling over weken voor het vaststellen van het tijdstip waarop de druivenoogst een aanvang kan nemen.

## XI

In het Jaar van de Vrouw (1975) dient bij promotieplechtigheden minimaal één van de twee paranimfen een vrouw te zijn.

## XII

Gelet op het belang van crèche en kleuterschool voor de ontwikkeling van het kind, verdienen de namen van deze opleidingsinstituten een vermelding in het curriculum vitae van een promovendus.

De schrijver van dit proefschrift werd op 2 november 1945 te Nijmegen geboren. Vanaf 1950 tot 1960 woonde hij te Deventer, alwaar hij de lagere school en twee klassen van het gymnasium doorliep. Hierna keerde hij terug naar zijn geboortestad. Als leerling van het Stedelijk Gymnasium behaalde hij het eind-examen  $\beta$  in 1963. September van dat zelfde jaar begon hij, daartoe door zijn ouders in de gelegenheid gesteld, scheikunde te studeren aan de Katholieke Universiteit te Nijmegen. Het candidaatsexamen SI werd met goed gevolg afgelegd op 5 juni 1967. Hoofdvak in zijn doctoraalprogramma was reactiekinetiek en katalyse op de afdeling van Prof.Dr.Ir.J.W.E.Coenen, als bijvak werd gekozen biofysische chemie op de afdeling van Prof.Dr.G.A.J. van Os.

Intussen trad hij in maart 1969 in het huwelijk met Clementine Tuijl Schuitemaker en woonde één jaar in het landelijke Lent, om daarna weer terug te keren naar Nijmegen.

Op 12 januari 1970 werd het doctoraalexamen behaald. Hierop volgde een aanstelling als wetenschappelijk medewerker verbonden aan de afdeling Katalyse voor het bewerken van een proefschrift. Met achtereenvolgens Dr.Ir.H.Th.Rijnten en Dr.Ir.J.H.Kaspersma werd met veel plezier samengewerkt in het opbouwen van de apparatuur en het bespreken van de meetresultaten.

Twee zonen werden hem geschonken door Clementine: Acmon in 1970, Floris in 1972.

R.Z.C. van Meerten, Postweg 123, Nijmegen, The Netherlands.



